IMPACT OF THE BUILT ENVIRONMENT ON MICROCLIMATE IN SAN JOSÉ, CALIFORNIA

A Thesis submitted to the faculty of
San Francisco State University
In partial fulfillment of
the requirements for
the Degree

Master of Arts

In

Geography: Resource Management and Environmental Planning

by

Reese Noel Hann

San Francisco, California

December 2020

CERTIFICATION OF APPROVAL

I certify that I have read Impact of the Built Environment on Microclimate in San José, California by Reese Noel Hann, and that in my opinion this work meets the criteria for approving a thesis submitted in partial fulfillment of the requirement for the degree Master of Arts in Geography: Concentration in Resource Management and Environmental Planning at San Francisco State University.

Andrew Oliphant, Ph.D.
Professor,
Thesis Committee Chair / Date

Sara Baguskas, Ph.D.
Assistant Professor / Date

Impact of the Built Environment on Microclimate in San José, California

Reese Noel Hann
San Francisco, California
2020

Most cities have heterogeneous land uses, which produce internal variability in the Urban Heat Island (UHI). Urban heating coupled with rising global temperatures leads to an increase in heat-related illnesses, decrease in human comfort and increase in energy consumption. This study investigates the spatial variability of the UHI at the neighborhood scale in San José, California using a mobile transect to measure temperature differences. Sampling sites were classified into Local Climate Zones (LCZ) based on vegetation, impervious fractions, and building morphology. Average evening temperature differences were 1.5 °C warmer downtown than an urban park and 0.5 °C cooler in a well vegetated neighborhood compared to neighborhood with similar built urban form, but different amounts of vegetation. Stronger wind speeds decreased temperatures differences between LCZs. Results are consistent with theory that vegetation provides cooling via evapotranspiration and that increases in the built urban form lead to increases in temperature. LCZs with increased impervious and building surface fractions experienced increased temperatures whereas LCZs with increased pervious fractions experienced cooler temperatures.

PREFACE AND/OR ACKNOWLEDGEMENTS

This research was created out of my love for San José, observations made from my own front yard, and the communities affected by the differences in temperature. I will always be looking out for socioeconomic and environmental justice for the most vulnerable peoples.

Thank you to all the special people and family who supported me and made my research possible.

- To Andrew Oliphant, who has taught me so much and has been ever patient. He took on my research proposal, born out of our love for climatology and my tenacious interest in urban planning and the intersection of the science which informs our decisions.
- To Michael Breidert who used his amazing GIS skills to make this research using the LCZ system possible. He created maps and provided us with the geospatial analysis of characteristics in the built urban form of San José.
- And to my spouse, Adrian De La Cerda, who drove me around in a manual transmission car on city streets, in stop and go traffic, for 24 transects at all times of the day. Adrian has been constant support throughout my education and is the reason I am here today.

TABLE OF CONTENTS

LIST OF TABLES

Table Page

LIST OF FIGURES

LIST OF APPENDICES

Introduction

Urban areas are becoming more densely populated globally (United Nations (UN), 2018). Of the world's population, 54% live in urban areas and this number is expected to increase to 66% by 2050 (UN, 2018). As urban populations increase, there is usually an increase in the built urban form, i.e., buildings, parking lots, etc., which change the landscape and impact city temperatures (Kleerekoper et al., 2011). Urban planning, which address increases in density, urban form, and population should integrate climate into their conversation as these modifications alter the climate regimes in cities (Gago et al., 2013). Each city needs individual analysis to identify each microscale climate differences, which is unique and affected by specific characteristics in the built urban form. Urban development plans, whether for future development or renovations of space, should factor in microclimate in order to optimize public use of space (Kleerekoper et al., 2011).

The Urban Heat Island (UHI) effect is the result of changes in the surface energy budget due to replacement of the natural environment by the built environment (Oke, 1987). Intra-urban UHI studies seek to explain temperature differences based on the built urban form and sample different urban environments. These samples address different levels of heating based on urban design factors such as building height, amount of vegetation, or spacing between buildings. Planning and mitigation efforts should be informed by an understanding of which urban design factors affect the UHI and Human Thermal Comfort (HTC). HTC is a measurement at the scale of the human body, which is used to understand felt temperature and the experience of a person in a particular place (Oke, 1987).

HTC will be affected by climate change in addition to urban form. Climate change models based on two different emission scenarios project an increase in temperatures from 2.4 °C to 4.3 °C by 2100 (Dahl et al., 2019). Under both emissions scenarios, the annual number of days with heat indices exceeding 37.8 °C (100 °F) and 40.6 °C (105 °F) are projected to double and triple, respectively, compared to a 1971–2000 baseline (Dahl et al., 2019). In July of 1995, there were a total of 514 heat related deaths with an additional 254 deaths likely caused by heat in Chicago, Illinois (Whitman et al., 1997). This increase in heating coupled with the UHI leads to an increase in intensity and frequency of heat waves which are linked to extreme heat related illnesses and increased mortality rates (Bowler et al., 2010).

The UHI is defined as the air temperature differences between urban and surrounding rural landscapes: UHI=T_u-T_r, where T_u is urban air temperature and T_r is rural air temperature (Oke, 1987). In most regions, the comparative rural landscape is comprised of permeable surfaces, increased surface water storage, and vegetation similar to the city site in its pre-urban natural state (Oke, 2006). Vegetation promotes evapotranspiration, a key process in cooling the surrounding area, as plants absorb solar radiation and transform this energy into latent heat rather than sensible heat via transpiration (Bowler et al., 2010). Shade from trees cools the microclimate by intercepting solar radiation, which reduces warming on the ground surface or of the surrounding air (Bowler et al., 2010). Therefore, areas with more vegetation and soil, such as urban parks, can produce cool air pools within a broader UHI driven by higher evapotranspiration rates (Bowler et al., 2010). The Park Cool Island (PCI) is defined as PCI=T_u-T_p, where T_u is urban air temperature and T_p is park air temperature (Spronken-Smith & Oke, 1998).

The built urban form is constructed with a variety of materials, most of which have different thermal and radiative properties than the previously existing landscape (Morgan et al., 1977). These urban materials store much greater amounts of heat during the day and release that heat at night causing urban areas to be warmer than surrounding rural regions, particularly in the hours after sunset (Terjung & Louie, 1973). However, not all urban areas worldwide have the same UHI due to the vast differences in materials, form, weather conditions, climate, vegetation, and building density. Other than differences in the urban form and materials, the amount of vegetation, soil and surface water in a city directly impacts the amount of moisture in the air (Terjung et al., 1970). Additionally, anthropogenic activities, such as running air conditioning or driving cars, add heat to the city scape (Iamarino et al., 2012).

The built urban form of a city alters the Surface Energy Balance (SEB), defined as:

$$Q^*+Q_F=Q_H+Q_E+\Delta Q_S, \text{ (Eq. 1)}$$

where Q^* is net allwave radiation, Q_F is the anthropogenic heat flux, Q_H is the sensible heat flux, Q_E is the latent heat flux, and ΔQ_s, the change in heat storage (Oke, 1987). In a city, Q_H and ΔQ_S, are typically larger and Q_E smaller than in surrounding rural energy budgets (Morgan et al., 1977; Oke, 1987). The reduction in vegetation and soil water storage decreases Q_E, which reduces cooling of a region via evapotranspiration (Gunawardena et al., 2017). The additional energy this provides during the middle of the day enhances both Q_H and ΔQ_S, which warms the urban surface layer atmosphere. This increase in Q_H and ΔQ_S in cities directly increases warming causing the UHI.

Cities also experience an increase ΔQ_S due to more heat penetrating the urban materials during the day when Q^* is high (Oke, 1987). The increase in ΔQ_S is caused by greater absorption of solar radiation due to radiation trapping and reflection by building walls and vertical surfaces. This reduces daytime convective losses in the canopy layer which are instead delayed and released at night (Stewart & Oke, 2012). The thermal properties of typical building materials absorb incoming radiation whereas vegetation has lower temperatures due to evapotranspiration and the conversion of incoming radiation instead of absorption (Shashua-Bar & Hoffman, 2000).

The anthropogenic heat flux, Q_F, is derived from three main human activities: in buildings from heating or air conditioning systems, transportation, and from human metabolism (Iamarino et al., 2012). In the greater London area in England, the average annual anthropogenic heat flux was 10.9 W m^{-2} in 2005-2009, a minimal amount compared to incoming daily solar radiation which ranges by latitude in the hundreds of W m^{-2} (Iamarino et al., 2012).

As the SEB changes across urban form, so does the temperature. The SEB changes between neighborhoods that vary in the amount of vegetation. Areas with higher vegetation cover have a higher ratio of Q_E to Q_H which can lead to a cooling of the surrounding environment (Oke, 1987). Areas with increased Q_H are produce higher temperatures and a higher UHI (Oke, 1987). Cities are complex and comprised of all these variations in the built urban form.

The terms ‘urban’ and ‘rural’ are too limiting when studying UHI in cities as each individual area of a city has unique physical properties which contribute to a microclimate that is distinct from other areas or neighborhoods of the same city (Stewart & Oke, 2012). Previous UHI studies, which typically surveyed simple temperature differences between urban and rural areas, missed the complexity of the built urban form in a city and the factors which either add or mitigate heat (Oke 2006). To better understand the microclimate differences within a city, the

UHI became more commonly evaluated in terms of temperature differences between different types of urban form or density, such as in Nagano, Japan (Sakakibara, & Matsui, 2005), Tel Aviv, Israel (Shashua-Bar & Hoffman, 2000), and Singapore (Wong & Yu, 2005). These studies addressed temperature differences based on vegetation, population and built density, and city zoning. In Japan, researchers were interested in the connection between densely inhabited districts (DID) and the effect of this built urban form on the UHI. It was found in six settlements, city size indices and DID are highly correlated to temperature differences between urban and rural landscapes.

In Israel, a summer survey was conducted to collect temperature data from 11 urban green areas with trees to analyze the cooling effect of trees and found an average of 2.8 K cooler in urban green areas with trees with a range from 1 K to 4 K (Shashua-Bar & Hoffman, 2000). In 2005 in Singapore, researchers identified urban form differences such as the airport, forest, residential, and industry and conducted a mobile transect to identify temperature differences across the city (Wong & Yu, 2005). A connection was found between lower temperatures and vegetation while densely built urban forms such as the CBD (Central Business District) had the highest temperatures (Wong & Yu, 2005).

Additionally, in some cities it is difficult to find a rural representative area. The rural-urban boundary continues to expand with development and population growth. The boundary can also be contained by valleys and/or water bodies, such as the study site of this research, San José, California. This is problematic when obtaining UHI values as the goal is to avoid extraneous microclimate influences, and the thermal properties of water and increases in elevation such as orographic effects are met with changes in temperature due to physical geography rather than differences in the built urban form compared to the previous natural environment (Oke, 2006).

Due to the complex form of cities, the Local Climate Zone (LCZ) Classification framework was proposed in 2012, which identifies differences in the built urban form and land cover types within cities to measure the intra-urban variability of the UHI (Stewart & Oke, 2012). This framework permits LCZ comparisons relative to the overall city temperature, which helps identify UHI magnitude differences within each distinct zone. The LCZ classifications are based on geometric and surface cover properties including, but not limited to: sky view factor (SVF), aspect ratio, building surface fraction, impervious and pervious surface fraction, height of roughness elements, and terrain roughness class using Davenport et al.'s (2000) classification for city and country landscapes (Stewart & Oke, 2012).

LCZs are split into ten built types, which are commonly found in the urban form worldwide (Figure 1)(Betchel et al., 2017). These range in density, stories, size, natural or constructed materials, and use (Stewart & Oke, 2012). There are seven LCZ based on land cover types, which are natural landscapes (Stewart & Oke, 2012). These include dense trees, scattered trees, brush or scrub, low plants, bare rock or paved, bare soil or sand, and water (Figure 1)(Betchel et al, 2017). There are also four ephemeral land cover properties to account for seasonal differences: snow cover, bare trees, dry ground, and wet ground (Stewart & Oke, 2012).

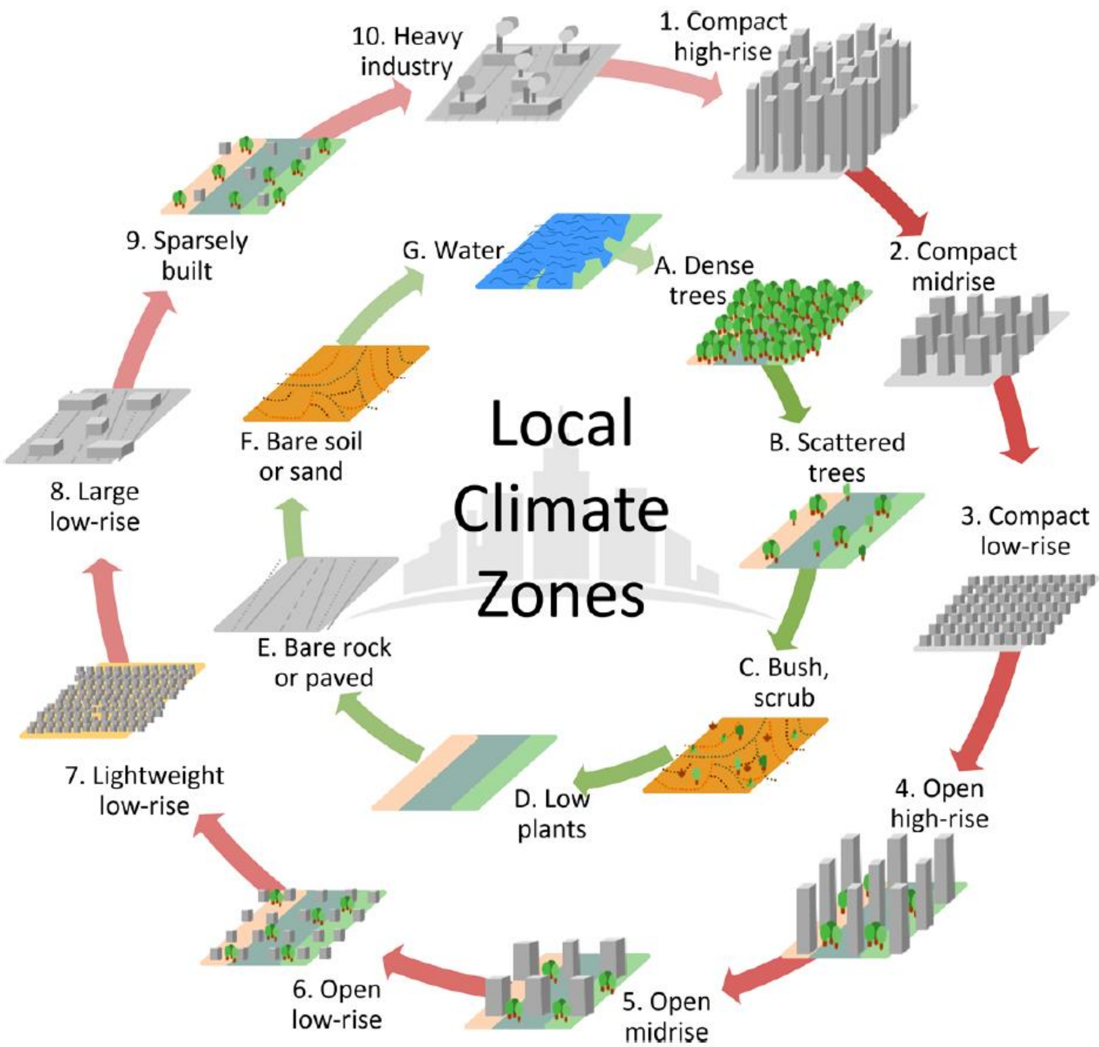

Figure 1: LCZ classification types. LCZ 1-10 represent built urban forms while LCZ A-F represent natural land cover properties. Figure taken from Betchel et al.,(2017, p.4).

Classifying LCZs consists of collecting metadata and defining the thermal source area. Metadata can be collected via site visits, but more often now, metadata is collected from datasets obtained from and collected by local agency or municipalities, governmental organizations, nonprofits, or from ESRI, the Environmental Science Research Institute. These datasets are analyzed using geographic information systems (GIS) which consists of land cover/land use maps, aerial photographs, and satellite imagery (Stewart & Oke, 2012).

Defining the thermal source area of each LCZ is imperative as the source area is the region monitored or observed by the temperature sensor, often called the footprint or circle of influence (Oke, 2006; Stewart & Oke, 2012). The source area determines if the designated region is representative of the LCZ classification. Consideration of the thermal source area includes wind direction as a key factor. The source area should extend upwind from the instrumentation for accurate temperature measurements of a designated LCZ (Oke, 2006). There are 10 measurements suggested by Stewart and Oke (2012) to determine LCZ classification. However, studies use varying amounts of the measurements with most using between five to eight, (e.g., Stevan et al., 2013; Alexander & Mills, 2014; Thomas et al., 2014; Leconte et al., 2015; Lehnert et al., 2015; Wang et al., 2016; Skarbit et al., 2017; Yang et al., 2017; Kotharkar & Bagade, 2018; Aminipouri et al., 2019).

The LCZ regime was meant to classify structures, such as buildings, trees, or housing, worldwide based on their climatic properties (Betchel et al., 2015). The classification system is meant to be inherently generic yet contain select well-engineered features so that it may cover cities across climates and ecoregions worldwide (Demuzere et al., 2019). Local differences in cities such as the layout of city streets, cultural differences in the density and spacing of buildings, historic design styles, vegetation, types, and buildings materials are not considered in the framework (Betchel et al., 2015). The framework encourages users to create subclass sites which deviate from the standard set and represent a combination of built or land cover types (Figure 2) (Stewart & Oke, 2012; Demuzere et al., 2019). Due to variances in the built urban form worldwide, subclassification of LCZ is common among studies which find some of their measurements lie outside of the indicators of a specific class. Multiple LCZ studies subclassify built urban forms and natural landscapes in a means to communicate the differences in city structure e.g., (Leconte et al., 2015; Lehnert et al., 2015; Yang et al., 2017; Kotharkar & Bagade, 2018; Perera & Emmanuel, 2018; Anjos et al., 2020). In Colombo, Sri Lanka, 46 distinct LCZs were found during a mapping campaign derived from the standard set and the application of subclasses (Perera & Emmanuel, 2018).

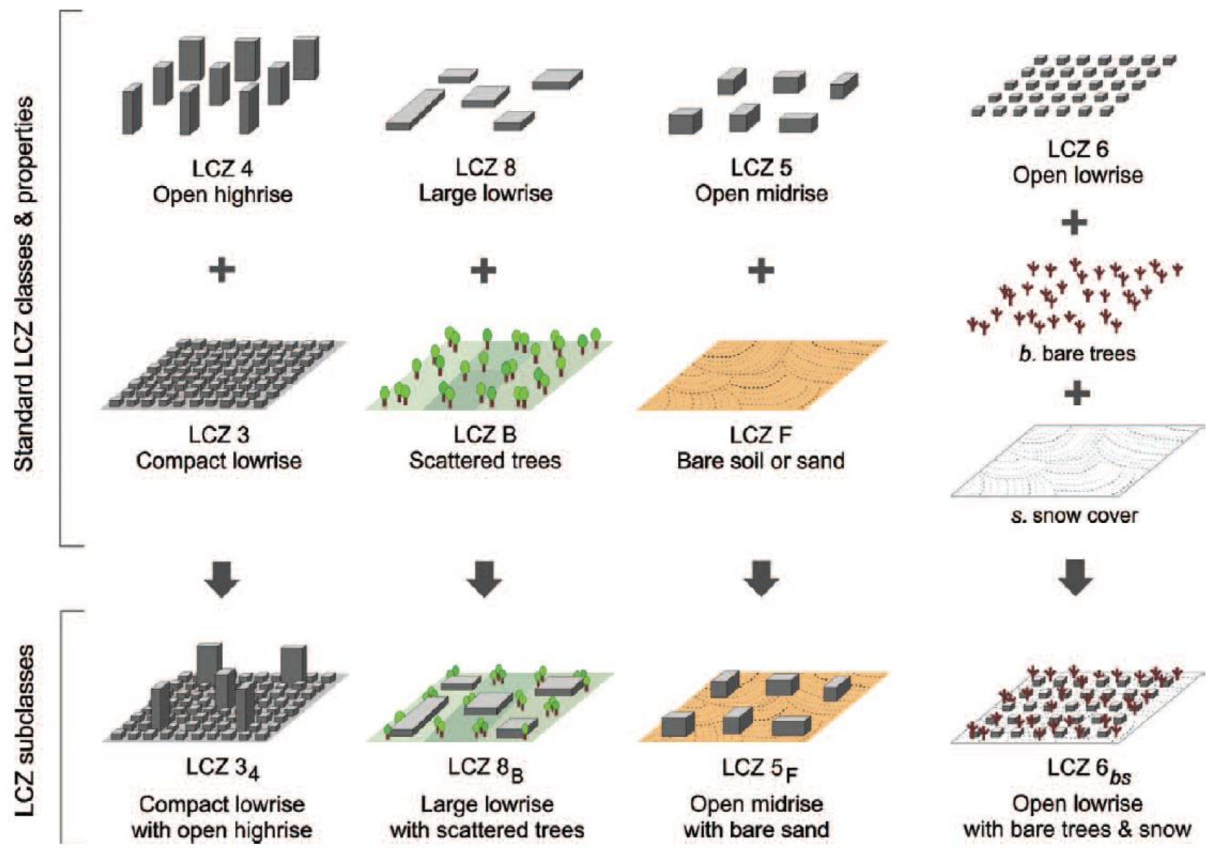

Figure 2: Local Climate Zone subclassification process. Figure taken from Stewart & Oke (2012, p. 14).

Currently, there are multiple ways in which studies report LCZ findings. Often reported values are UHI magnitudes or intensity. Studies which report these values choose a LCZ, usually the coolest in temperature, and report the UHI from the chosen LCZ as a reference. Differences from the LCZs collective average temperatures are most common and most desirable to use when completing inter-city comparisons. When inter-city comparison is lacking, the single city analysis of average temperature differences between LCZs is applied as $\Delta Tair_{LCZ\ x\text{-}y}$. In $\Delta Tair_{LCZ\ x\text{-}y}$ reporting, there is no city average. Reporting of differences between LCZs is difficult to use in inter-city comparisons as it only works if the city in question has the same LCZs as the city in the study. Some studies also report average temperature of each LCZs and compare each LCZ average against another LCZ temperature average in their study. This reporting can be used, although it does not provide a temperature difference from an average and therefore can be difficult to apply in inter-city comparisons.

Table 1: Collection of studies with multiple LCZs similar to San José with temperatures taken after sunset. Temperature difference, UHI magnitude, UHI intensity, and temperature averages based on reporting method of selected study.

LCZ 1	LCZ 2	LCZ 8	LCZ 6	LCZ A/B	LCZ D	LCZ G	Reference
3.1 K	3 K	1.8 K	1.2 K	-0.2 K		2 K	(Yang et al., 2017) Nanjing, China **UHI Magnitude**
	3.13 °C		1.92 °C				(Thomas et al., 2014 Kochi, India **UHI Intensity**
			0.3 °C	24.8°C*		24.8 °C*	(Chieppa et al., 2018) Auburn, AL, USA **UHI Intensity**
			1.4 °C	24.9 °C*		26 °C*	(Chieppa et al., 2018) Opelika, AL, USA **UHI Intensity**
2.5 K		0.8 K	(-0.4) K	(-0.6) K (-1) K	(-2.6) K		(Stewart & Oke, 2012)

LCZ 1	LCZ 2	LCZ 8	LCZ 6	LCZ A/B	LCZ D	LCZ G	Reference
							Vancouver, BC, Canada **Temperature Difference**
	2.1 °C		0.97 °C		(-2.17) °C		(Alexander & Mills, 2014) Dublin, Ireland **Temperature Difference**
0.7 °C	0.6 °C	0.4 °C			(-0.3) °C	(-0.8) °C	(Anjos et al., 2020) Londrina, Brazil **Temperature Difference**
		1.1 °C	0.3 °C	(-7) °C	(-3.5) °C	0.4 °C	(Wang et al., 2018) Las Vegas, NV, USA **Temperature Difference**
		1.2 °C	(-0.1) °C	(-0.5) °C	(-2) °C	(-0.8) °C	(Wang et al., 2018) Phoenix, AZ, USA **Temperature Difference**

*Chieppa et al. (2018) did not report water or forest temperatures as a UHI intensity, only average temperatures which were not statistically significant from the LCZ 6.

Table 2 is a selection of LCZ studies which had two or more LCZs that are also found in San José, California. Generally, LCZs 1, 2, and 8 have higher temperatures, temperature differences, or UHI magnitudes than LCZ 6, open low rise development. In cities where LCZ 1, 2, and 8 were surveyed, LCZ 1 and 2 have higher temperatures, temperature differences, or UHI magnitudes than LCZ 8. Lowest temperatures, temperatures differences, or UHI magnitudes are found in natural landscapes A, B, D, or G (Table 2). These findings are consistent with the framework’s assessment of LCZs in Vancouver, BC, which shows that positive temperature departures occur in built urban forms and natural environments have negative temperature departures (Table 2)(Stewart & Oke, 2012).

These results indicate that higher temperatures are found in areas with increased built urban density including increases in building surface area and building surface fraction. The alteration of the surface energy balance in LCZs 1,2, and 8 causes a lack of evapotranspiration and an increase in energy absorption into building materials. These LCZ study results also show that areas with vegetation or water, produce cooler temperatures due to evapotranspiration and pervious land cover, which is found in the form of natural environments. These findings are consistent with theory of the UHI and PCI effect; changes from the natural environment to the built environment cause warmer temperatures. Similarly, in LCZ 6s surveyed in Table 2, only two reported temperatures below average, but still not equal to temperature differences in LCZs A-G.

An advanced search on Google Scholar (https://scholar.google.com/) procures publication data from 2012, the initial publishing of the LCZ framework, to 2020, showing that there are over 1,250 results which mention LCZs and the Urban Heat Island using a Boolean search function. These articles range from reviews, case studies, models, classification best practices and more. According to Xue et al. (2020), there have been over 800 citations of the original framework and publication of over 220 articles in 2019 alone. Xue et al. (2020) attributes this growth due to the diffusion of urban climatology into applied fields such as urban and regional planning, building and construction technology, engineering, and ecology concluding that LCZ classification addresses more than urban temperature; rather it is a gateway to sustainable urban development and human health.

Due to the wide range of applicability and interest in the LCZ scheme, mobile measurement case studies are not well represented in the LCZ literature. Out of 610 articles published and analyzed about the LCZ classification scheme, only 109 focused on the surface urban heat island, land surface temperature, MODIS (Moderate Resolution Imaging Spectroradiometer), and the urban heat island effect (Xue et al., 2020). Within these 109 articles, methods such as MODIS can be used to evaluate temperature using imagery rather than field measurements. The four most popular publication categories in LCZ literature other than the UHI effect included: 1. OTC (outdoor thermal comfort) and PET (physiologically equivalent temperature), 2. remote sensing and convolutional neural networks, 2. SUEWS (Surface Urban Energy and Water Balance Scheme) and WRF (Weather Research and Forecasting Model), and 4. Crowdsourcing air temperature, cyber-infrastructure, and citizen weather station (Xue et al., 2020).

In an analysis of 50 cities using the LCZ investigating surface UHI, there was no city studied with a Csb Köppen climate classification. (Bechtel et al., 2019). Additionally, all these cities from the 50 city comparison used MODIS instead of field measurements to assess the UHI. The dominate Köppen climate classifications surveyed in the 50 city comparison were Cfa, Cfb, Dfa, Dwa, Dfb, and Aw, most of which are represented in Table 2, which compares LCZ results from studies using field methods (Betchel et al., 2019). Additionally, Las Vegas, NV and Phoenix, AZ have a classification of Bwh and are represented since Arizona State University is the leading institution publishing LCZ related literature with over 112 publications as of July 2020 (Xue et al., 2020).

With relatively limited examples of field measurements and a lack of representation of Mediterranean climates, San José, California provides a good example of a Csb Köppen climate classification, which is a warm summer Mediterranean climate. This case study adds to the collection of LCZ literature addressing a particular climate regime and adds a sample of built urban forms and their temperature deviations from San José.

The broader objective of this study was to investigate the spatial variability of ambient air temperature at 2 m at the neighborhood-scale in San José, California, USA during summer. Specific objectives were to obtain detailed temperature differences between neighborhoods using a mobile measurement system, and to characterize the local climate zone of each using the Stewart and Oke (2012) LCZ classification system. Additionally, temperature samples were taken in the afternoon and morning to identify changes over the diurnal cycle. Analysis was conducted asking how temperature responds to heat events and how temperature changes due to differences in wind speed.

This study explores variability in the built urban form and amount of vegetation to reveal temperature differences and patterns of the LCZs caused by land use in urban environments within the same city. This information will be compared with similar LCZ studies conducted in other cities with different climates, but similar built environments. We aim to place the San José findings in the context of intra-urban temperature measurements made in comparative neighborhoods worldwide which use the LCZ classification system to draw broader conclusions about urban heating and the implications for planning further urban growth.

We hypothesize that expected results would include higher temperatures in the minimally vegetated neighborhood compared to the highly vegetated neighborhood regardless of similar urban form. Additionally, the highest overall temperature in the city is expected to be produced by densely built urban form, the downtown region. Temperature differences will be greatest following sunset, weakened during windier conditions, and strengthened under hotter background weather conditions.

Methods

2.1 Study Area

This research was conducted in San José California, USA, located at 37 °N and 122 °W, which is a conurbation of the San Francisco Bay Area (Figure 3). San José is the third largest city in California and 10th largest in the US with a population of 1,046,079 persons as of January 1, 2017 and growing at a rate of 0.9% annually (Department of Planning, 2014). San José is located in a Mediterranean climate (Köppen Csb), with warm to hot, dry summers and mild to cool, wet winters. Annual total rainfall is approximately 400 mm, with less than 3% falling during summer months. Average daily maximum temperature for June through September is approximately 27 °C (National Climate Data Center). An ‘extreme heat day’ for San José is considered to be equal to or greater than 34.28 °C (Cal Adapt, 2020).

Figure 3: Map of the San Francisco Bay conurbation in California with San José located in the South. Maps obtained from the City of San José open GIS data and maps (2020).

San José covers an area of 460 km^2 on a wide, flat section of the Santa Clara Valley, between the Diablo Mountain Range to the east and the Santa Cruz Mountains to the west, and San Francisco Bay to the north (Figure 4). Winds generally come from the north and northwest during the day in summer, driven by regional-scale north-westerlies, which are channeled down San Francisco Bay. This is coupled with a local-scale sea breeze and valley winds, also producing northerly airflow during the day. At night, winds are frequently reversed to blow down valley (southerlies) when drainage flows are coupled with a land breeze (Miller 1999). The large flat area of San José provides a useful location for comparing temperature variability as a function of the built environment because the effects of individual land use types on temperature can be isolated from topographic controls.

Figure 4: Topographic imagery of the relief in the San Francisco Bay Area with San José situated in the south valley. Imagery provided by Michael Breidert.

2.2 Instrument Design

Measurements were made during mobile traverses across the city using an instrumented passenger vehicle. The vehicle was fitted with T-shaped PCV pipe, attached to the roof rack (Figure 5). The structure raised the measurement height to 2 m, 32 cm above the vehicle roof and the horizontal pipe channeled airflow directly to the sensors. In the center of the PCV pipe, exposed to the channeled airflow was a type-E thermocouple and a Vaisala HMP60 thermistor and hygristor (Vaisala Inc, Helsinki, Finland). Vehicle mounted sensors were at 1.8 m above ground level, aspirated both naturally by vehicle motion and using a 12V fan, positioned at the rear of the PVC tubing so as to continuously draw air from the front of the tubes past the sensors. Attached to the outside of the PVC pipe pointing laterally to the right of the car, an Apogee thermal infrared radiometer (Apogee Instruments Inc., Logan Utah) was mounted. The radiometer was directed towards surfaces to the right of the vehicle capturing the built urban environment, such as houses, parkland, or buildings, which the vehicle passed by.

The instruments were wired into a CR1000 Campbell Scientific data logger (Campbell Scientific Inc. Logan, Utah), which was programmed using Loggernet software. The datalogger recorded air temperature from the type E thermocouple and HMP60 thermistor, relative humidity from the HMP60 hygristor, and surface temperature from the infrared radiometer. The datalogger was programmed with a sampling frequency of one second, and each study area was sampled for three minutes for a total of 180 samples.

Figure 5: Vehicle with Mounted PCV pipe containing the type E thermocouple, HMP60 thermistor hygristor, Apogee infrared radiometer, and 12-volt fan.

The same instruments were used in each transect and each study site. Assuming instrument error is small and systematic, it is unlikely to play a role in the inter-site differences observed in this study. However, in order to check instrument performance prior to data collection, the instruments were compared with three other similar sensors on a campus rooftop for one week, storing 10-minute averages derived from one-second samples. The instruments responded to temperature and humidity differences equivalently over the period, with mean absolute differences <0.3 °C for the thermistor, <0.15 °C for the thermocouple and <2.5% for relative humidity observed by the hygristor. In all cases the coefficient of determination between the instruments used in this study and their comparison sensors was greater than 0.98.

2.3 Mobile Transect

Mobile measurements were collected along 24 transects between June 2019 and August 2019 during the following time periods: 17 in the evening following sunset (2100-2300 PDT), five during the early afternoon (~1400 PDT) day, and two in the early morning (~0400-0500). Each of the six LCZs was sampled by driving continuously within the designated area at a speed of approximately 50 km h^{-1} for three minutes (Figure 6). For the park and lake sites, due to access constraints at evening, observations were made while the vehicle was parked at the downwind border of the parklands (assuming the prevailing NW flow). Each transect took approximately 45 to 70 minutes to conduct.

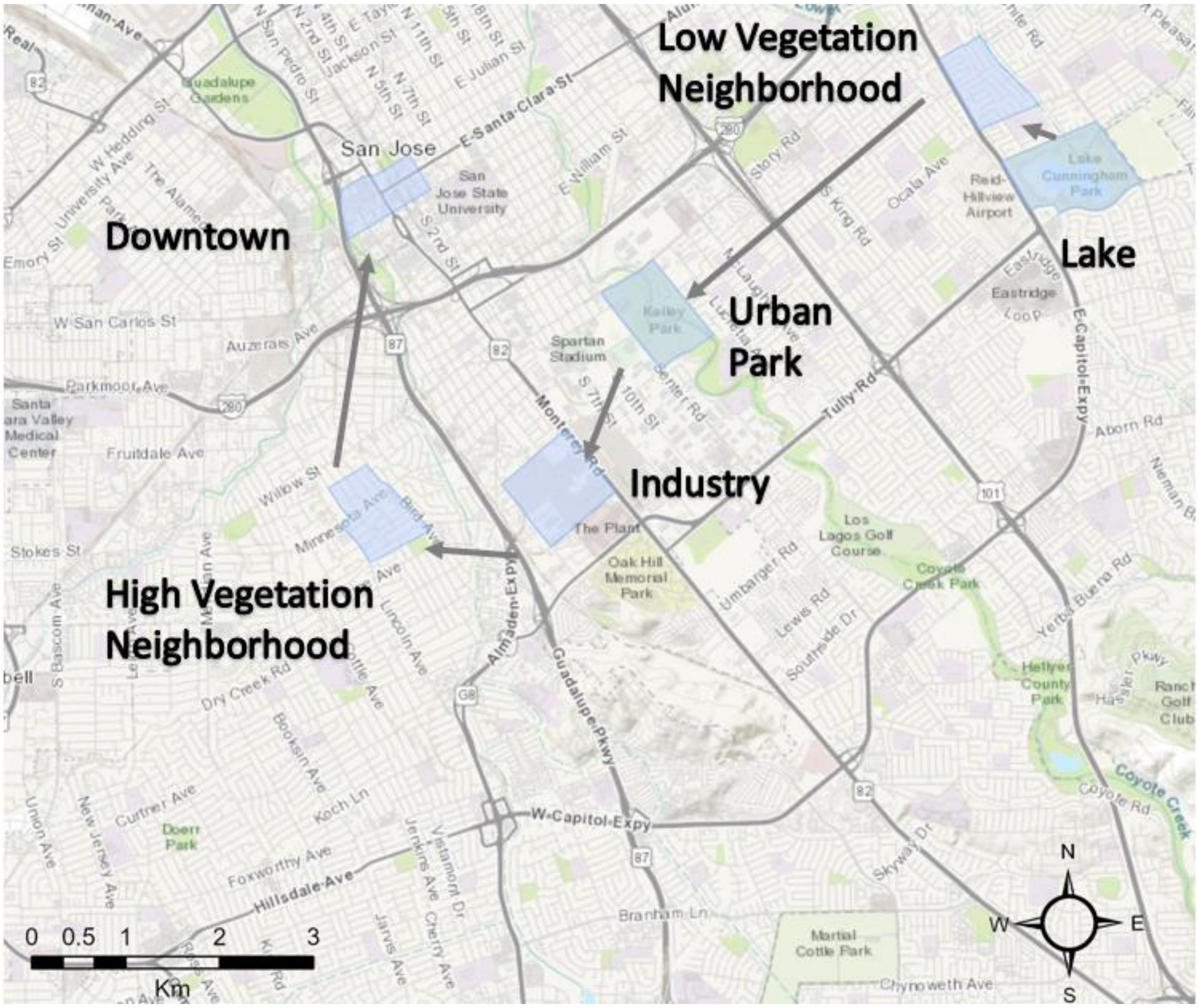

Figure 6: Map of LCZ locations in San José. Transect route occurred East to West beginning at the lake and ending downtown. Map provided by Michael Breidert.

2.4 Local Climate Zone Classification

LCZ classification for San José used Google Earth and ArcGIS to determine the characteristics of the urban form. Each LCZ underwent analysis of five geometric and surface cover properties: aspect ratio, building fraction, impervious fraction, pervious fraction, and average element height (Table 2).

Table 2: Measurements and definitions of properties required to classify LCZs. Rows 1-7 represent geometric and surface cover properties. Rows 8-10 represent thermal, radiative, and metabolic processes (Stewart et al., 2012).

	Measurement	Definition from Stewart & Oke (2012)
1	Sky View Factor	Ratio of the amount of sky hemisphere visible from ground level to that of an unobstructed hemisphere
2	Aspect Ratio	Mean height to width ratio of street canyons in LCZ 1-7, building spacing in LCZ 8-10, and/or tree spacing in LCZ A-G
3	Building surface fraction	Ratio of building plan area to total plan area
4	Impervious Surface Fraction	Ratio of impervious plan area to total plan area
5	Pervious Surface Fraction	Ratio of pervious plan area to total plan area
6	Height of roughness element	Geometric average of building heights and/or trees
7	Terrain Roughness class	Davenport classification of effective terrain roughness
8	Surface Admittance	Ability of surface to accept or release heat
9	Surface Albedo	Amount of solar radiation reflected by a surface
10	Anthropogenic Heat Output	Mean annual heat flux density

The spacing of urban elements for the aspect ratio was obtained using the ruler function in Google Earth in all LCZs. In each LCZ, more than 30 random sample observations were obtained for spacing between either buildings, trees, or street canyons. Additionally, element height for trees was obtained from Google Earth using the same methodology. To obtain the aspect ratio in the urban park and lake, tree element height average was divided by tree spacing average to obtain the aspect ratio.

The element height for buildings, however, was obtained from an open source building footprint GIS dataset from the City of San José. The average building height was found in each LCZ and was obtained by dividing the number of unique buildings by the total of all building heights in each LCZ. To obtain the aspect ratio in the downtown, both neighborhoods, and the industrial LCZs, the building element height average was divided by either street canyon width average or building spacing average.

The building surface fraction was obtained from the same data set as building heights by finding the total surface area of buildings in each LCZ. This total building area was then divided by the total area of each LCZ. This number was multiplied by 100 to obtain the building surface fraction as a percentage.

The impervious and pervious surface fractions data sets were obtained from the National Land Cover Database (NLCD) maintained by the Multi-Resolution Land Characteristics Consortium which includes partners such as the United States Geological Survey (USGS), the National Oceanic and Atmospheric Administration (NOAA) , the Environmental Protection Agency (EPA), and more. 30m resolution cells were designated with an impervious or pervious count. These cells were extracted for each LCZ and counted as a total sum. The cells were categorized as either pervious or impervious and divided by the sum and multiplied by 100 to find the percentage of pervious and impervious surface for each LCZ. Building surface fraction was subtracted from the impervious surface fraction to create the impervious ground surface fraction. The impervious ground, pervious ground, and building surface fraction equate to 100 percent of the total area of each LCZ.

In this study, five out of ten LCZ indicators were explored: aspect ratio, building surface fraction, impervious surface fraction, pervious surface fraction, and height of roughness elements. This study did not estimate five LCZ indictors which included: sky view factor, terrain roughness class, surface admittance, surface albedo, and anthropogenic heat output.

A higher parent class should represent the standard set and one or more classes can be assigned a subclass based on LCZ measurements (Stewart & Oke, 2012). This higher parent classification was assigned to each LCZ based on visual physical characteristics of the urban form and site measurements which were dominant in the LCZ region. Subclassifications, which represent secondary and tertiary characteristics of the built or natural urban forms, were found within our LCZs. These subclassifications were assigned based on the measurements which were outside of the indictors for the parent class assigned to each LCZ. LCZ subclassifications are ordered numerically by differences in the built urban form, 1-10, and then alphabetically by differences in the natural environment, A-G.

2.5 Temperature Corrections & Data Analysis

Due to the temporal changes in temperature over the duration of each transect, temperature corrections were required for accurate comparison between LCZs. In a similar study that used a mobile vehicle system to quantify air temperature variation in an urban area, Leconte et al. (2015) accounted for the natural variation in air temperature by applying a linear time correction using the initial air temperature at the start of their sampling session as a reference temperature. Similarly, we used a linear regression model to account for the natural temperature change based on each transects starting temperature. Figure 7 shows the one-second temperature samples from a single transect captured after sunset. A linear decrease in temperature can be observed, associated with the early nocturnal cooling part of the diurnal cycle (blue line, Figure 7). A linear regression model (orange line) was fit to the variation in temperature in order to find the linear rate of change over the transect. This rate of cooling was used to correct all samples observed after the initial sample (purple line), which was used to assess the relative temperature differences between LCZs.

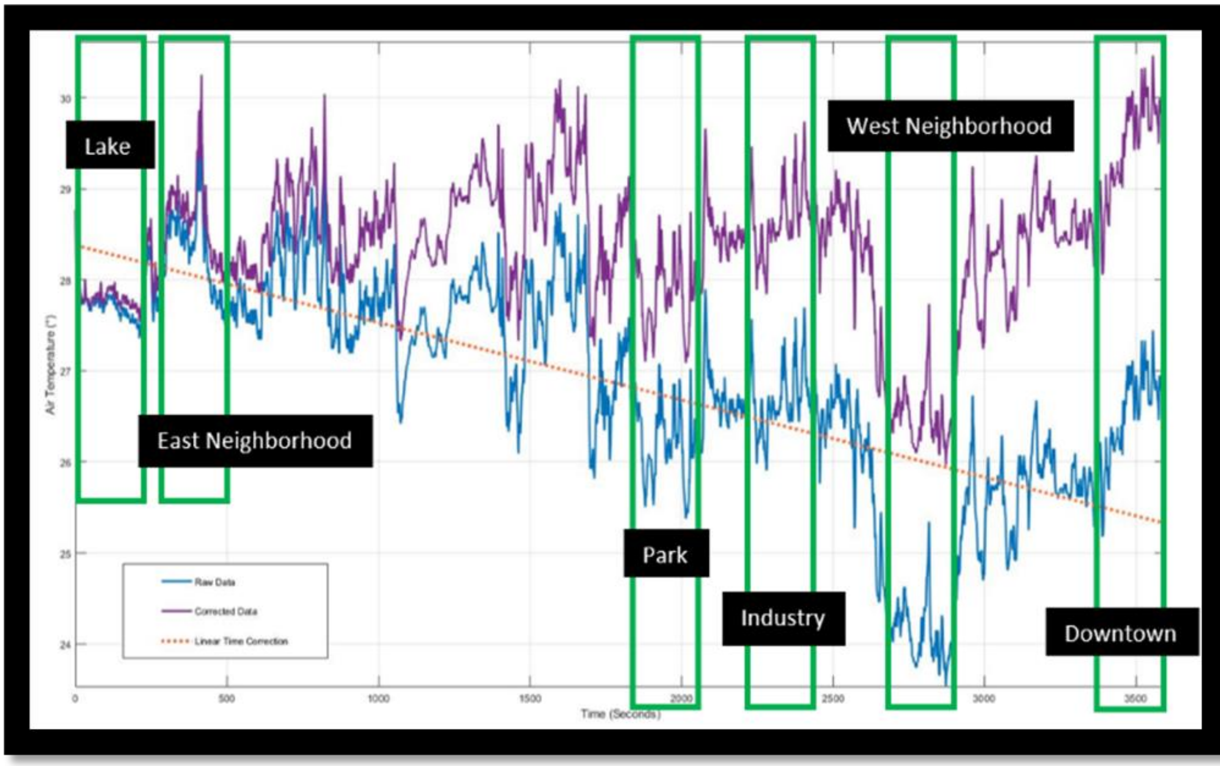

Figure 7: Raw temperature data, corrected data, and linear time correction for a transect collected on July 27th, 2019 from 21:10 to 22:09 with the LCZ measurement sites indicated by the green boxes.

Meteorological data was also downloaded from the MesoWest network of automated weather stations for a station located at the San José Airport, which provided fixed 5-minute average meteorological data over the entire study period. These data were used to derive background meteorological conditions during each transect, so that inter-LCZ climate differences could be evaluated with respect to wind speed and direction, background temperature and humidity.

MATLAB, an analysis software which uses matrix and array programming, was used to process the data obtained from a total of 24 transects. For the two fixed measurement sites, the urban park and the lake, the instruments were stationary and located to the South Southeast. Therefore, observations only represented the intended LCZ for wind directions between 285° and 30° due to the location of the measurement site relative to the LCZ. There were 13 evening transects with North to Northwest wind directions and all five afternoon transects also had North to Northwest winds. All six LCZs were analyzed when the wind direction was between 285° and 30°.

Analysis of all 17 evening transects regardless of wind direction was also conducted but excluded the lake and the urban park. These four LCZs, which did not need wind direction as a consideration for accurate representation of their built urban forms, were the open high vegetation neighborhood, open low vegetation neighborhood, downtown midrise, and the light industry zone. Additionally, we examined the diurnal patterns of the six LCZs on two days in late July 2019.

We compared air temperature between the different LCZs and the average temperature of the city which was calculated as average air temperature per transect to estimate city-wide temperature during each measurement session. The variability in the magnitude of UHI per LCZ was calculated as the difference in air temperature between a given LCZ and the average mean of all the LCZs sampled. This LCZ average replaces a rural reference site and shows the difference between city temperature and neighborhood scale temperature (LCZs).

Investigation of the data collected also consisted of examining each location's variability to determine the range of temperatures within each location. To test for statistical differences in evening temperature between sites, we performed an Analysis of Variance (ANOVA) and post-hoc Tukey test using statistical software (RStudio, version 4.0.2).

Results

3.1 Classifying Local Climate Zones in San José

Classification of the urban form in San José illuminated that many values of geometric and surface cover properties fell outside of the LCZ scheme indicators. The built urban form is innately complex, leading to differences that cannot be fully covered by the standard set of LCZ framework (Betchel et al., 2015). Therefore, the framework authors suggest subclassification of LCZs to account for the differences in built urban form (Stewart & Oke, 2012). All six LCZs in San José experience more than one value lying outside of the indictor provided by the LCZ classification framework for the geometric and surface cover properties we surveyed (Table 3 & Table 4). For two of the LCZs, we applied a single subclass to designate vegetation differences in the open low rise neighborhoods. Additionally, the urban park received a single subclass of E, bare rock or paved. For the downtown compact midrise and the lake, we have added two additional subclasses to represent the differences seen in the urban form.

Table 3: Visual physical characteristics of LCZ classifications from Stewart & Oke and site selections in San José, California (2012). Aerial satellite imagery provided by Michael Breidert (2020). Classification graphics retrieved from Stewart & Oke (2012). Eye level photos taken from Google Earth street view.

Classification	Aerial Satellite Imagery	Eye Level Photo
G. Water 		
6. Open low-rise 		
B. Scattered trees 		
8. Large low-rise 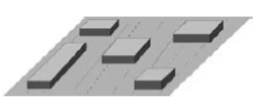		
6. Open low-rise 		

Classification	Aerial Satellite Imagery	Eye Level Photo
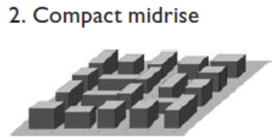		

Table 4: LCZ names, classifications, physical properties, site measurements, and the LCZ indicators for each classification according to Stewart & Oke (2012). Pervious, impervious, and building percentages obtained by Michael Breidert. Aspect ratio and average element height obtained by Michael Breidert, Andrew Oliphant, and Reese Hann.

LCZ Name	LCZ Class	Properties	Site Measurements	LCZ Indicator
Lake	G_{BE}	Aspect Ratio % Building % Impervious % Pervious Element Height (m)	0.08 0.7 20.3* 79* 12.2*	<0.1 <10 <10 >90 -
Open Low Vegetation Neighborhood	6_E	Aspect Ratio % Building % Impervious % Pervious Element Height (m)	0.14* 26.1 69.4* 4.5* 3.7	0.3-0.75 20-40 20–50 30-60 3–10
Urban Park	B_E	Aspect Ratio % Building % Impervious % Pervious Element Height (m)	0.73 1.8 22.2 76 16.2*	0.25–0.75 <10 <10 >90 3–15
Light Industry	8	Aspect Ratio % Building % Impervious % Pervious Element Height (m)	0.17 31.3 67.7* 1 4.8	0.1–0.3 30–50 40–50 <20 3–10
Open High Vegetation Neighborhood	6_B	Aspect Ratio % Building % Impervious % Pervious Element Height (m)	0.25* 27.3 5.7* 67* 4.5	0.3-0.75 20-40 20–50 30-60 3–10

LCZ Name	LCZ Class	Properties	Site Measurements	LCZ Indicator
Downtown Compact Midrise	2_{1E}	Aspect Ratio	0.76	0.75-2
		% Building	39.7*	40–70
		% Impervious	55.3*	30–50
		% Pervious	5	< 20
		Element Height (m)	20.3	10-25

*denotes value is outside of the LCZ indicator for its classification

The lake is a part of a park, with a pay to enter waterpark in the Northwest corner. Due to dependence on automobiles in San José, there is an abundance of parking space. The urban park area contains paved barbeque pits and gazebos and also includes the water park structures. On the Southeast corner of the lake, there is also a paved skate park. All of these factors explain the larger impervious surface fraction of 20.3% and a decreased pervious fraction of 79% which lead to a subclassification of E, bare rock or paved surface (Table 4). There are trees inside of the park with additional trees lined along most of the park perimeter to create a barrier between street traffic and the park. This caused the supplemental subclassification B, scattered trees, with an average element height of 12.2 (Table 4).

The urban park in San José also has an increased impervious surface fraction of 22.2% and a decreased pervious fraction of 76% which caused a subclassification of E, paved or bare rock (Table 4). The park has a Japanese garden on the eastern side and a history park in the South with multiple historical buildings representing the past of San José and the cultures which settled in this region. The park also has a large parking lot in the Northeast corner since the northern area of the park is a pay to enter small zoo with children's rides. Besides this parking lot, the urban park has three other paved parking lots which have caused the increase in the impervious surface fraction.

The open low vegetation neighborhood has a high impervious fraction of 69.4% and a small pervious fraction of 4.5% with the minimum range for the pervious fraction in this type of LCZ normally being 30% (Table 4). The subclass of E, paved or bare rock, was added to this neighborhood. There is an abundance of paved front yards in this LCZ and backyards also may be paved or covered in stone. Automobiles line the streets both day and night, with barely any space left to park. Driveways also have multiple parked cars, vans, or trucks. Where there is vegetation, it represents local plants, or occasional street trees.

The open high vegetation neighborhood has different urban form from the previously mentioned neighborhood. There is an abundance of vegetation including pervious front yards, smaller streets, and tree-lined avenues which called for a subclassification of B, scattered trees. In San José, this neighborhood has a high pervious fraction of 67% and a small impervious fraction of 5.7% with the minimum range for the impervious fraction in this type of LCZ normally being 20% (Table 4). Street parking is not as common in this area and many homes only use garage parking or may park a car or two on their driveway.

The industrial zone has a higher impervious percentage, 67.7%, than the indicator (Table 4). This region has many paved parking lots and streets in addition to large industrial buildings. Finding any pervious surface is a challenge with trees placed along only major arterial streets. This LCZ did not receive a subclassification even with a higher impervious percentage. The building percentage was within the indicator as well as the pervious, albeit the value was extremely low.

Downtown San José also has a higher percentage of impervious surfaces than the indicator totaling at 55.3% which caused a subclassification of E, bare rock or paved surface

(Table 3). The surveyed LCZ 2 in San José has no urban parks. However, downtown San José does have two urban parks, but these parks are located one block to the North and one block to the South of the LCZ. There are also a few open surface parking lots within this LCZ boundary, likely adding to the pervious fraction. While the building fraction is outside of the indictor, it only falls short by 0.3%, likely due to the increased surface parking instead of built garages or buildings (Table 3, Table 4). Downtown San José also received a subclassification of LCZ 1 for compact high rise. In this LCZ, midrise buildings are dominant, but there is a healthy mix of buildings over 10 stories (Table 3).

3.2 General Meteorological Conditions during the Field Study

Conditions during the 24 transects were typical of late summer conditions, dry and warm with occasional hot days, and winds typically from the north to northwest during the day and evening and from the south in the early morning (Figure 8). Wind speeds ranged from 1.2 m s^{-1} to 6.3 m s^{-1}, and average temperatures ranged from 14.7 °C to 33.6 °C during the study period. (Figure 8). Winds were consistently from the west to north except during two early morning transects when weak down-valley flow existed with wind direction from the south to southeast for Transects 23 and 24 (Figure 8). Most temperatures were typical of the summer in the mid 20 °Cs, but on a number of occasions, the temperatures reached greater than 30 °C even during the evening transects. The early morning transects were significantly cooler.

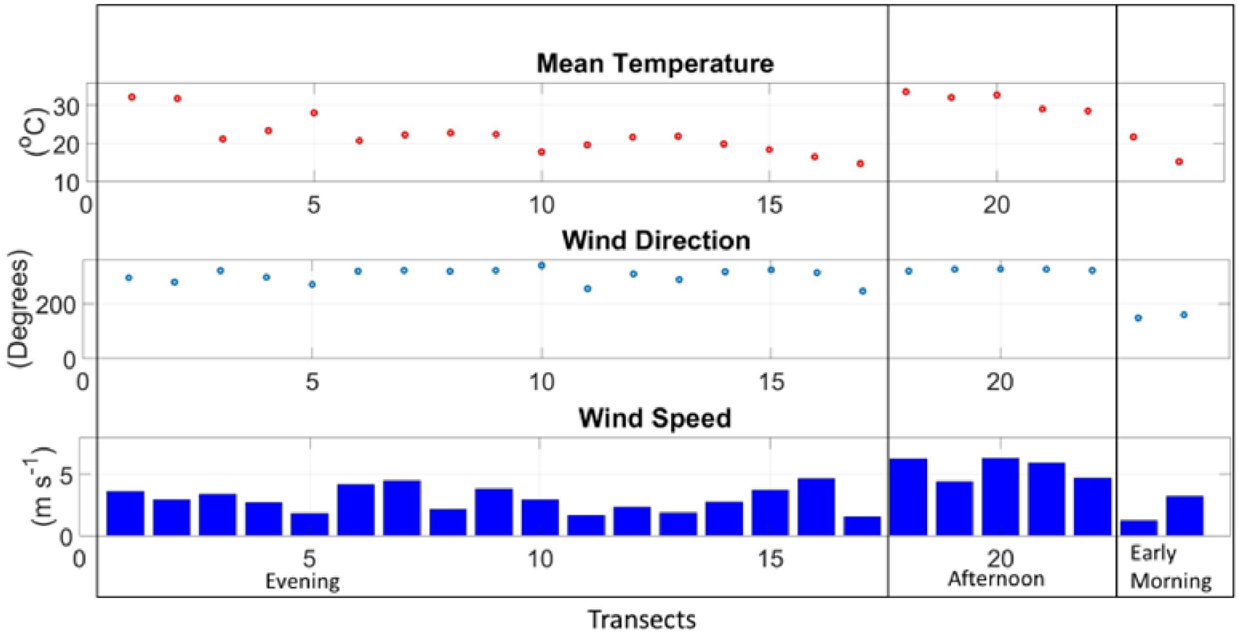

Figure 8: General wind direction (azimuth degrees), wind speed (m s^{-1}), and temperature (° C), conditions during the 24 transects. Transects 1-17 occurred in the evening, 18-22 surveyed in the afternoon, and transects 23 and 24 occurring in the early morning.

Wind direction in San José is typically from the North to Northwest, greater than 285° and less than 30°, during the day and early evening. Wind direction during this study for afternoon and evening transects was quite consistent and ranged from 246° to 339°.

3.3 Temperature Differences Observed between the LCZs

The deviation of each LCZ from the mean temperature of San José's site mean is shown in Figure 9. Here the temperature deviation refers to the differences between the 3-minute mean corrected temperature of each study site and the average of all six study sites. Transects with wind direction outside of San José's typical North to Northwest flows were only included in average temperature calculations for comparison between four LCZs, downtown midrise, open high vegetation neighborhood, open low vegetation neighborhood, and the light industry, which did not need these winds for a representative sample of their land use and urban form.

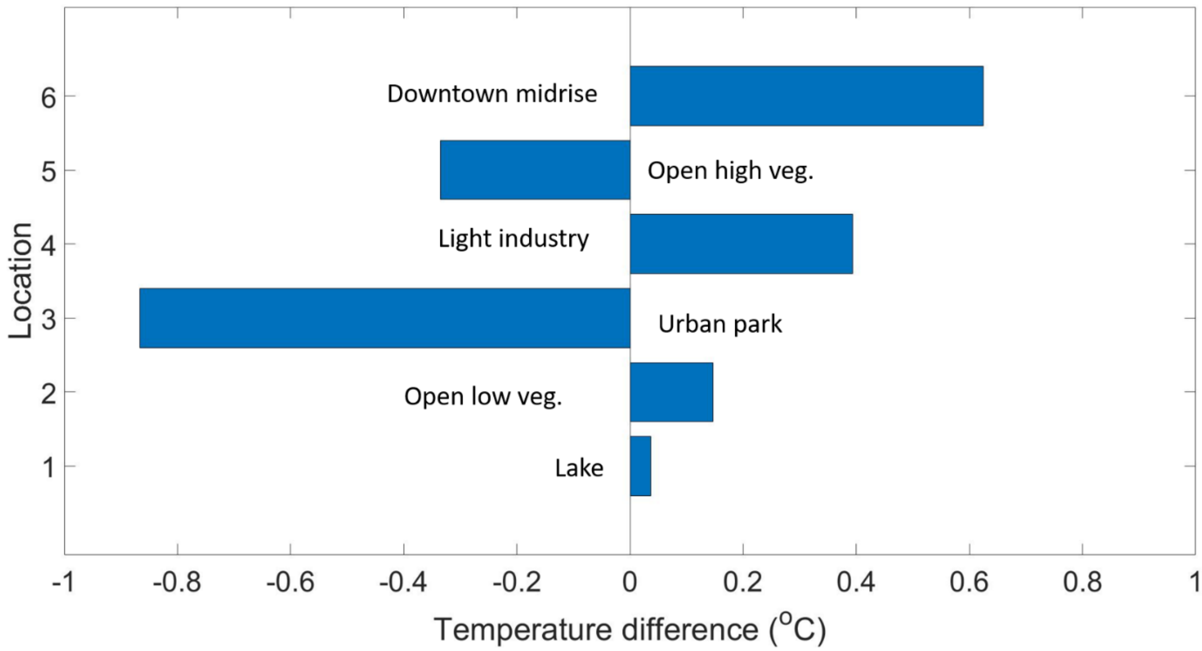

Figure 9: Mean evening temperature departure for each LCZ location. The transect mean was obtained for 13 evening transects surveyed with a wind direction from the North or Northwest.

Generally, there are positive values in four of the six LCZs while the urban park and open high vegetation neighborhood LCZs both experience lower than average temperatures (Figure 9). The maximum difference in ambient air temperature occurred between the urban park and the downtown midrise at 1.5 °C, with the downtown midrise experiencing the warmest temperatures in San José at 0.6 °C above the transect average (Figure 9). The light industry zone was the second warmest location with a temperature deviation of 0.4 °C and 1.3 °C higher than the urban park. The open low vegetation neighborhood was 0.5 °C warmer than the open high vegetation neighborhood. The two neighborhoods were classified in the same LCZ (Table 3), but the warmer site has 62.5% less vegetation by area. The lake in the evening was near the average of all sites and was 0.94 °C warmer than the urban park and most similar to the open low vegetation neighborhood.

The coolest temperatures were found in the two most vegetated zones. The urban park was the coolest zone at 0.9 °C below the average of the city, while the open high vegetation neighborhood was approximately 0.3 °C cooler than the city average. The temperature difference in the open high vegetation LCZ caused temperatures to be on average 0.5 °C cooler in this neighborhood than the open low vegetation LCZ.

Afternoon temperature departure patterns in four of the six LCZ were opposite of their evening values such as the hottest evening LCZ, downtown midrise, producing cool afternoon temperatures, 0.6 °C below the city average (Figure 10). Similarly, the urban park was not the coolest LCZ like in the evening, rather it was the hottest with a positive value of 1.3 °C above the city average (Figure 10). The lake produced the coolest temperatures in the afternoon with an average temperature difference from the mean of 1.4 °C contrary to its evening value which was slightly above the city average (Figure 10). The temperature difference between the urban park in the afternoon and the lake was 2.7 °C.

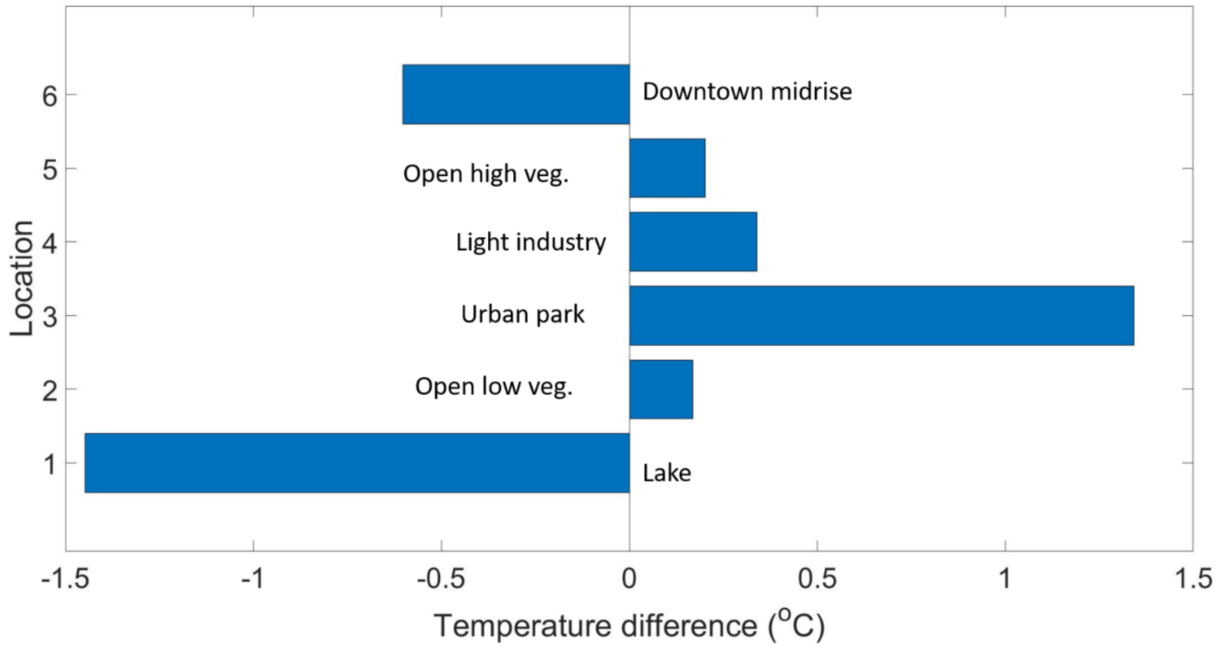

Figure 10: Mean afternoon temperature departure for each LCZ location. The site mean was obtained from five afternoon transects surveyed with a wind direction from the North or Northwest.

The open high vegetation neighborhood was similar to the open low vegetation neighborhood in the afternoons, unlike in the evenings, producing a positive temperature departure of 0.2 °C (Figure 10). The open low vegetation neighborhood was barely cooler than the high vegetation neighborhood, slightly warmer than the city average at 0.16 °C (Figure 10), which was similar to its temperature difference at night of 0.15 °C (Figure 9). The lake was 1.6 °C cooler on average than the open neighborhoods. Likewise, the light industry zone produced a warm afternoon temperature average of 0.34 above the city average (Figure 10), close to its evening value of 0.4 °C (Figure 9).

When wind direction was excluded at night, the downtown and industry LCZs both increased their temperatures, while the open neighborhoods decreased their temperatures (Figure

11). In cases of four LCZs, the mean is derived from the total of all six LCZs. Temperature differences between the LCZs are unaffected however the magnitudes would be different if the mean was derived from only four LCZs. There is greater cooling or heating in LCZs which were already cooler or warmer from the city average in Figure 9. The downtown midrise strengthened its temperature departure by 0.13 °C and the open high vegetation neighborhood produced even cooler temperatures with an average temperature difference from the mean of -0.45 °C which was 0.12 °C cooler than the general results in Figure 9. The industrial and open low vegetation neighborhood only changed temperature average slightly, by 0.05 °C and 0.04 °C, respectively (Figure 11).

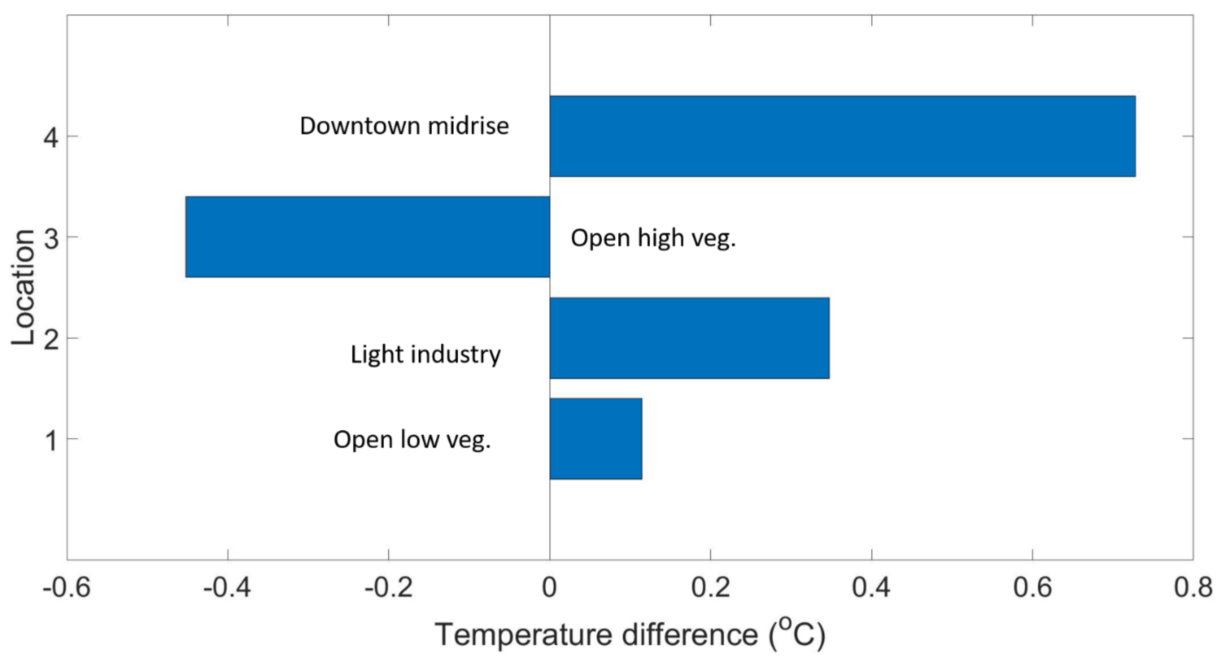

Figure 11: Mean evening temperature departure for four LCZ locations using all 17 evening transects from all wind directions.

3.4 Comparing Differences in Ambient Evening and Afternoon Temperature across LCZs

We found a statistically significant difference in temperature between most of the LCZ pairs ($P<0.05$). Ten out of the 15 possible LCZ pairs were statistically significantly different in the evenings and 11 of the 15 were different in the afternoon. (Figure 12 & Figure 13). The complete table of pairwise comparison of LCZs is provided in Appendix A and B.

The lake, which had a temperature departure closest to the mean in the evening samples, did not differ significantly from either open low rise neighborhood or the industrial LCZ ($P>0.05$, Figure 12). The industrial LCZ and open low vegetation neighborhood had high impervious percentage (67% and 69.4%, respectively) and did not differ significantly from one another. The downtown and industry LCZs were not significantly different from one another ($P>0.53$), which have similar building fraction percentages and high impervious percentages.

In the evenings, there were significantly different evening temperatures in the open vegetation neighborhoods, which also differed in pervious fractions with the open high vegetation neighborhood having 62.5% more pervious ground surface. The open low vegetation neighborhood was warmer than the open high vegetation neighborhood by 0.5 °C and this difference was significant ($P<0.008$). The evening temperature of the urban park was significantly different from all sites with the lowest temperatures in the evenings among all six LCZs ($P<0.05$). The open high vegetation neighborhood was 0.5 °C warmer than the park ($P<0.002$) while the open low rise was 1 °C warmer than the park ($P<0.0001$).

The downtown midrise LCZ was warmer than the urban park by 1.5 °C, and this difference was significant ($P<0.0001$). Furthermore, the downtown midrise LCZ had the highest temperatures and the urban park produced the coolest temperatures below the transect mean. These two LCZ had the largest temperature difference between any two LCZs.

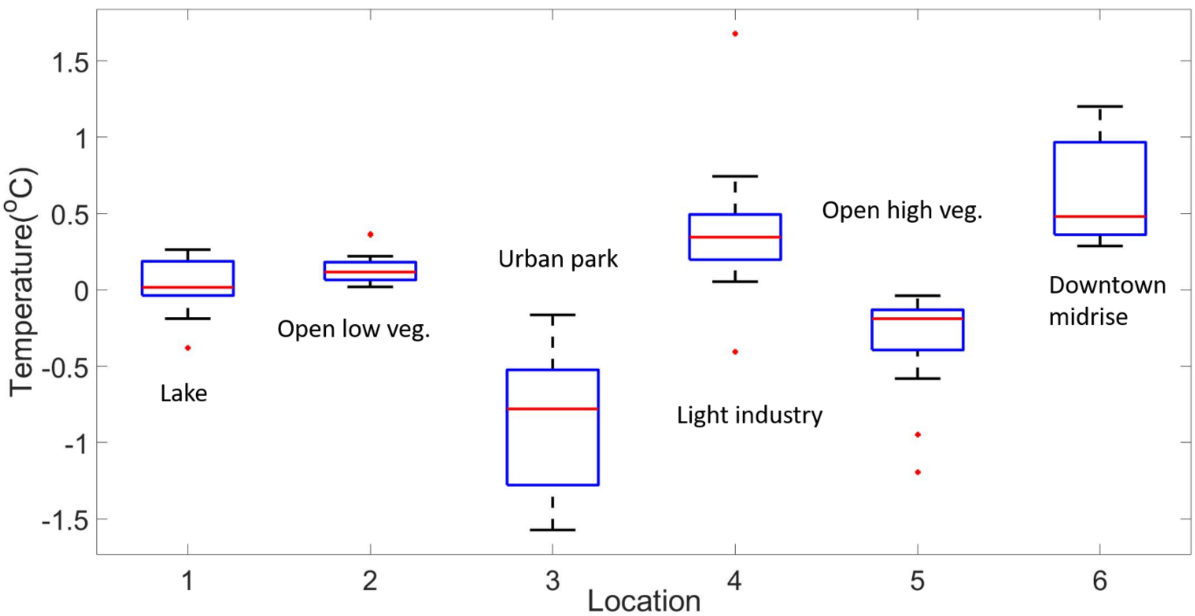

Figure 12: Box plots for each sampled LCZ showing the distribution of temperature variability for 13 evening transects with the wind direction from the North to Northwest. The LCZ average transect median (red line) is inside of the box. The top of the blue box represents the 75th percentile and the bottom represents the 25th percentile. The black lines extending from the boxes represent the tails of the temperature distribution and the red marks represent outliers.

In the afternoons, the open low vegetation neighborhood had a temperature departure closest to the mean and was not significantly different from the industry, downtown, or open high vegetation neighborhood. The industry LCZ was not significantly different than the open high vegetation neighborhood during the afternoon transects ($P<0.04$). The downtown midrise was the second coolest LCZ and was 0.9 °C cooler than the light industry LCZ, and this difference was significant ($P<0.012$).

Unlike in the evenings, the Lake afternoon temperature was statistically lower than all other LCZs. The afternoon lake temperature was 1.4 °C below the transect mean. The urban park had the warmest afternoon temperature and was significantly different from all other LCZs in the afternoons such as the downtown LCZ which was 1.9 °C cooler (P<0.0001). The lake was 2.9 °C cooler than the urban park, and this difference was significant (P<0.0001).

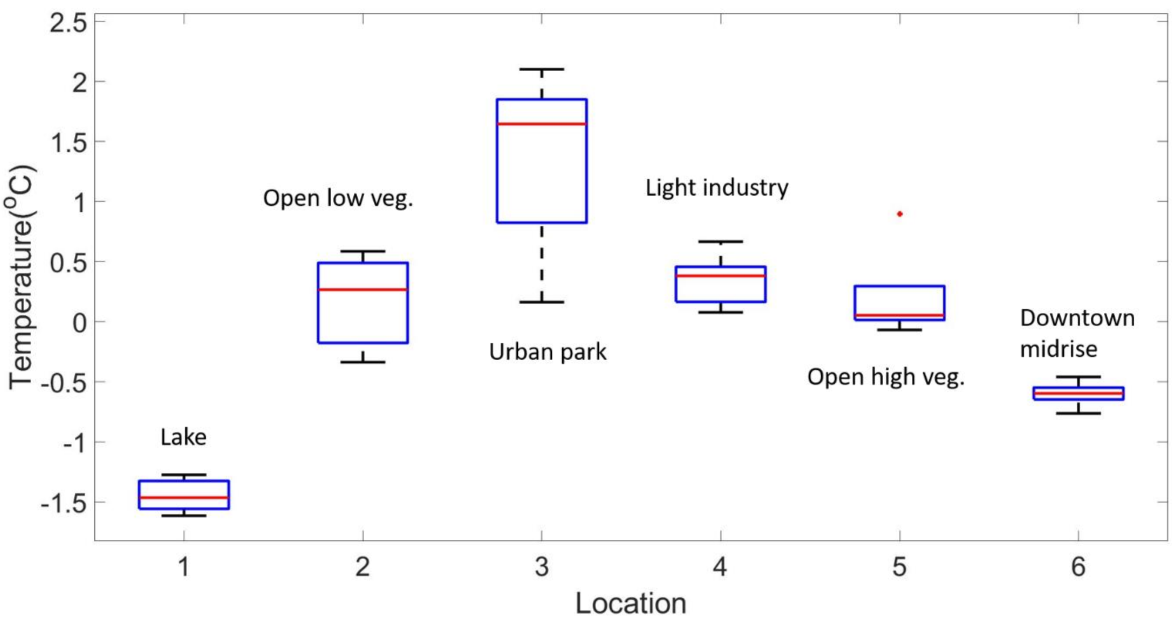

Figure 13: Box plots for each sampled LCZ showing the distribution of temperature variability for all five afternoon transects with the wind direction from the North to Northwest. The LCZ average transect median (red line) is inside of the box. The top of the blue box represents the 75th percentile and the bottom represents the 25th percentile. The black lines extending from the boxes represent the tails of the temperature distribution and the red marks represent outliers.

3.5 Comparing Wind Speed in the Evenings

Theoretically, UHI is strongest on calm evenings due to the decrease in advection and turbulent wind activity as weak winds and cloudless skies create the ideal conditions to trap heat in microclimates (Oke 1978). To examine windspeed, transects with windspeeds greater than the average of all evening transects were categorized as ‘windier’ evenings. Similarly, windspeeds less than all evening transect wind speed mean were categorized as ‘less windy’ evenings. Average temperature departures for windier transects (4.1 m s^{-1}) are compared with less windy transects (2.6 m s^{-1}) in Figure 14.

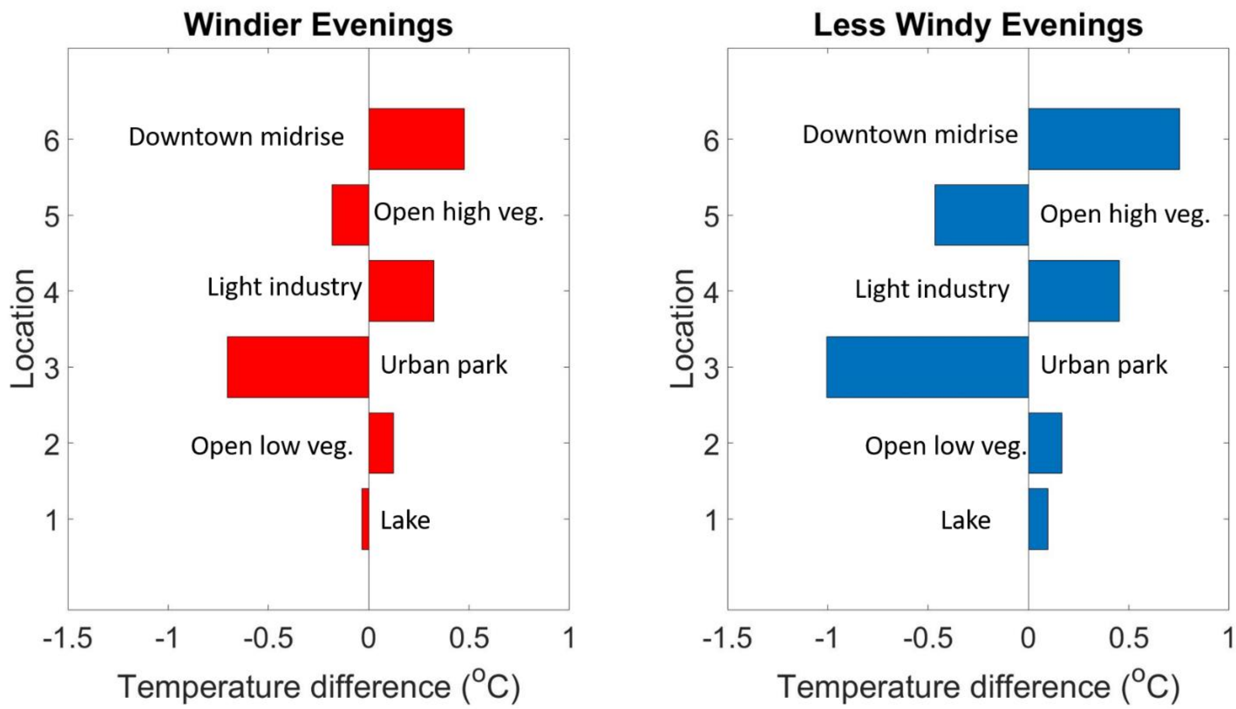

Figure 14: Mean temperature departure for 13 evening transects on 6 windier evenings and 7 less windy evenings. The site temperature mean was obtained for the 13 evening transects surveyed with North to Northwest wind direction. The average wind speed was 3.29 m s^{-1}. The average wind speed for windier evenings was 4.1 m s^{-1} and for less windy evenings, 2.6 m s^{-1}.

The patterns of temperature differences between sites remained similar to each other and those for the complete dataset in the evening with the downtown midrise showing the highest positive value and the urban park the coolest temperatures. The main difference appears to be that the temperature differences are enhanced under lower wind speeds. For example, the difference between downtown and the urban park was 1.19 °C under windier conditions and climbed to 1.75 °C under weaker winds.

Windier conditions weakened temperatures differences. The lake warmed on less windy evenings at 0.1 °C above the transect mean and showed a temperature departure of 0.03 °C below the average on windier evenings (Figure 14). On windier evenings, the difference between the open low vegetation neighborhood and the open high vegetation neighborhood was 0.3 °C while on less windy evenings, this difference was greater at 0.44 °C. The industry LCZ warmed from 0.33 °C to 0.45 °C on less windy evenings, an increase of 0.12 (Figure 14).

Without consideration for wind direction, Figure 15 shows the same pattern of weaker temperature differences during windier evenings. The temperature difference decreases between the open low vegetation and high vegetation neighborhoods on windier evenings with a difference of 0.3 °C. On less windy evenings, the temperature difference is increased to 0.71 °C between neighborhoods (Figure 15). The warming in the downtown midrise zone was almost double on less windy evenings, at 0.87 °C, while at 0.48 °C on windier evenings (Figure 15).

The industry LCZ barely changed temperatures under varying wind conditions, decreasing by 0.03 °C, from 0.36 °C on less windy evenings to 0.33 °C on windier evenings (Figure 15). However, the open high vegetation neighborhood has the same pattern as Figure 14 with an increased departure at 0.6 °C on less windy evenings and a weakened departure on windier evenings at 0.18 °C (Figure 15).

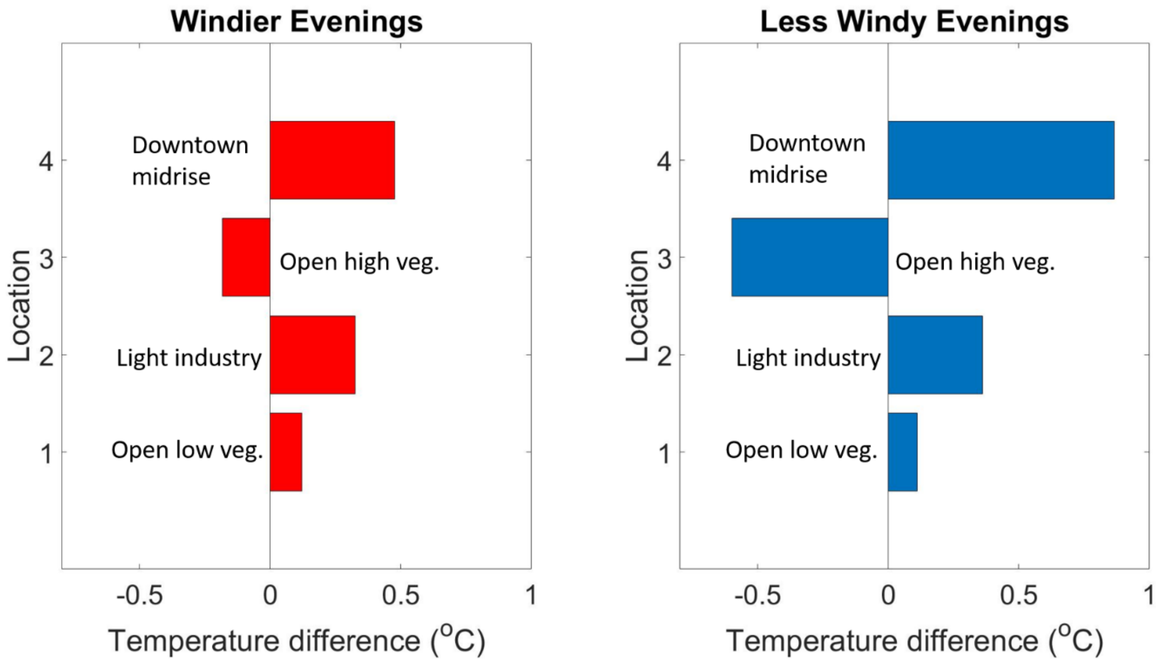

Figure 15: Mean temperature departure for four LCZ locations for 17 evening transects on 6 even windier evenings and 11 less windy evenings. The site temperature mean was obtained for all 17 evening transects surveyed. The average wind speed was 3 m s^{-1}. The average wind speed for windy evenings was 4.1 m s^{-1} and for less windy evenings, 2.4 m s^{-1}.

3.6 Impact of Ambient Temperatures on Temperature Departures

Theoretically, the UHI increases on hot evenings due to increased heating intensity and an increase in the absorption of heat into urban materials during the daytime hours. As it can be seen in Figure 16, most evening transect temperatures were between 18 and 24 °C. Here we compare the average of these cases with the one case when temperatures were consistently greater than 25 °C during the transect and winds were from the North to Northwest. The general pattern of evenings below 25 °C are similar to general results produced in Figure 9, whereas the single case above 25 °C has a unique pattern.

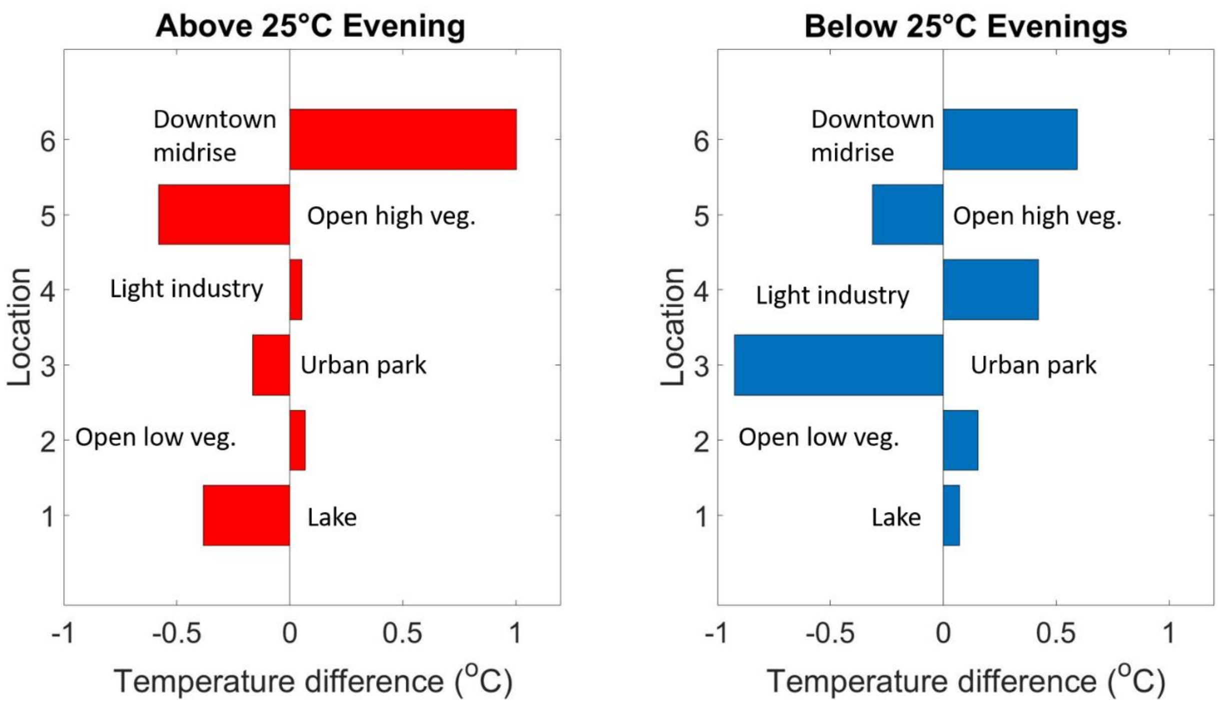

Figure 16: Mean temperature departure for each LCZ location on evenings with average temperature above or below 25 °C. The site mean was obtained from temperature transects with a wind direction from the North or Northwest. The mean transect temperature for the transect above 25 °C was 32.2 °C and on evenings below 25 °C the mean was 20.8 °C.

Temperature differences were strengthened in only two LCZs, the downtown midrise and open high vegetation neighborhood, under hotter background conditions. The downtown midrise zone increased in temperature by 0.4 °C and the open high vegetation neighborhood showed an additional 0.3 °C departure from 0.3 °C to 0.6 °C on the warm evening. The downtown was 1.6 °C hotter than the open high vegetation neighborhood on the evening above 25 °C, but only 0.9 °C hotter when temperatures were below 25 °C.

Temperature departures from the average weakened in the open low vegetation neighborhood, industry, and urban park on the evening above 25 °C. There is a low positive temperature departure in the urban park when temperatures are above 25 °C at 0.16 °C. On evenings below 25 °C, the urban park had a strong temperature departure at 0.93 °C, which is 0.77 °C cooler than on the evening above 25 °C. The industry zone gained 0.37 °C on evenings below 25 °C and the low vegetation neighborhood was strengthened as well, but only 0.08 °C on evenings below 25 °C. The lake experienced a little warming on evenings below 25 °C of only 0.07 °C while on the evening above 25 °C, the lake was 0.38 °C cooler than the average city temperature.

Excluding wind directions from the north to northwest, there were 3 transects with average transect temperature above 25 °C and 14 transects below 25 °C (Figure 17). These four LCZs follow similar patterns to the general results in Figure 9, with the downtown midrise being the warmest LCZ. Three LCZs, open high vegetation neighborhood, industry, and downtown midrise, had strengthened temperature departures under hotter background conditions.

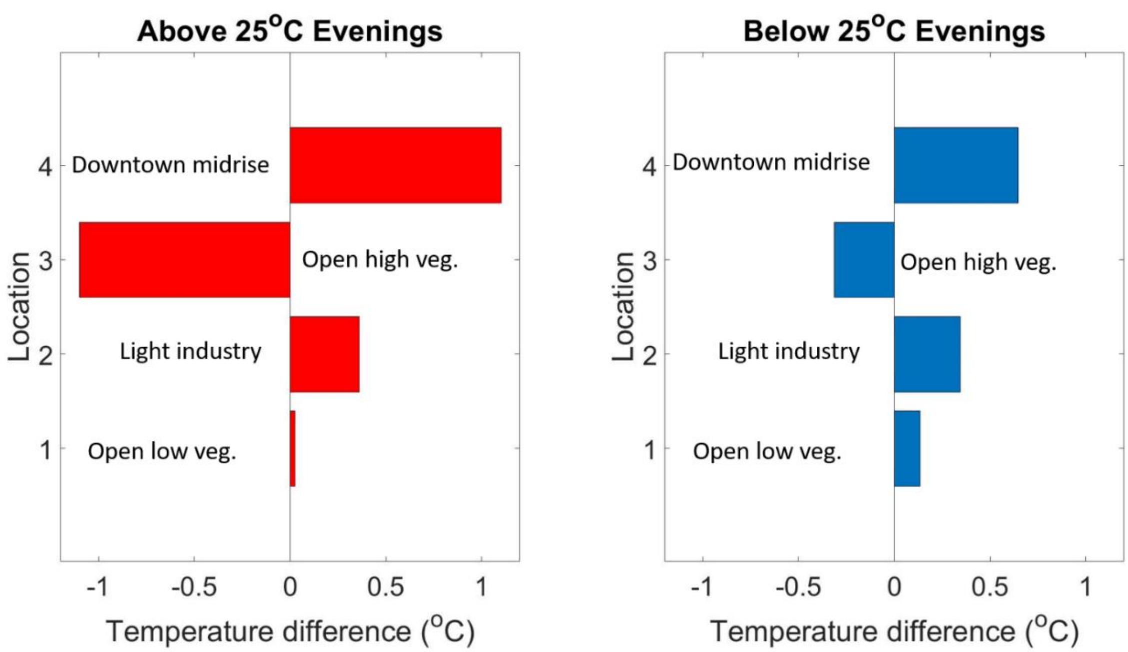

Figure 17: Mean temperature departure for four LCZ location on evenings with average temperature above or below 25 °C. The site mean was obtained from all 17 transects with all

wind directions. The mean transect temperature for evenings above 25 °C was 30.7 °C and on evenings below 25 °C the mean was 20.3 °C.

The downtown midrise zone saw the largest increase in warming by 0.45 °C to 1.1 °C on the evening over 25 °C and was 2.2 °C hotter than the open high vegetation neighborhood on evenings above 25 °C (Figure 17). On evenings below 25 °C, the difference was weakened to 0.96 °C. The light industry zone saw a minimal increase in warming of 0.01 °C on the evening above 25 °C (Figure 17).

The open low vegetation had a negligible change, but it experienced a slight decrease in temperature, 0.1 °C, on the evenings above 25 °C instead of the strengthened conditions seen in the other three LCZs (Figure 17). However, the temperature difference between the open low vegetation neighborhood and open high vegetation neighborhood was 1.13 °C hotter than on evenings above 25 °C and 0.44 °C hotter on evenings below 25 °C showing strengthened temperature differences under hotter background conditions.

3.7 Diurnal Variations in Temperature Departure

Two Saturdays in late July were surveyed three times per day to capture the diurnal variation in temperature across the LCZs. The winds were from the south for both morning transects, not allowing us to capture the lake and the park accurately. Therefore, analysis was conducted of the four LCZs which did not require North to Northwest winds for accurate temperature representation (Figure 18 & Figure 19). As with previous cases of four LCZs, the mean is derived from the total of all six LCZs.

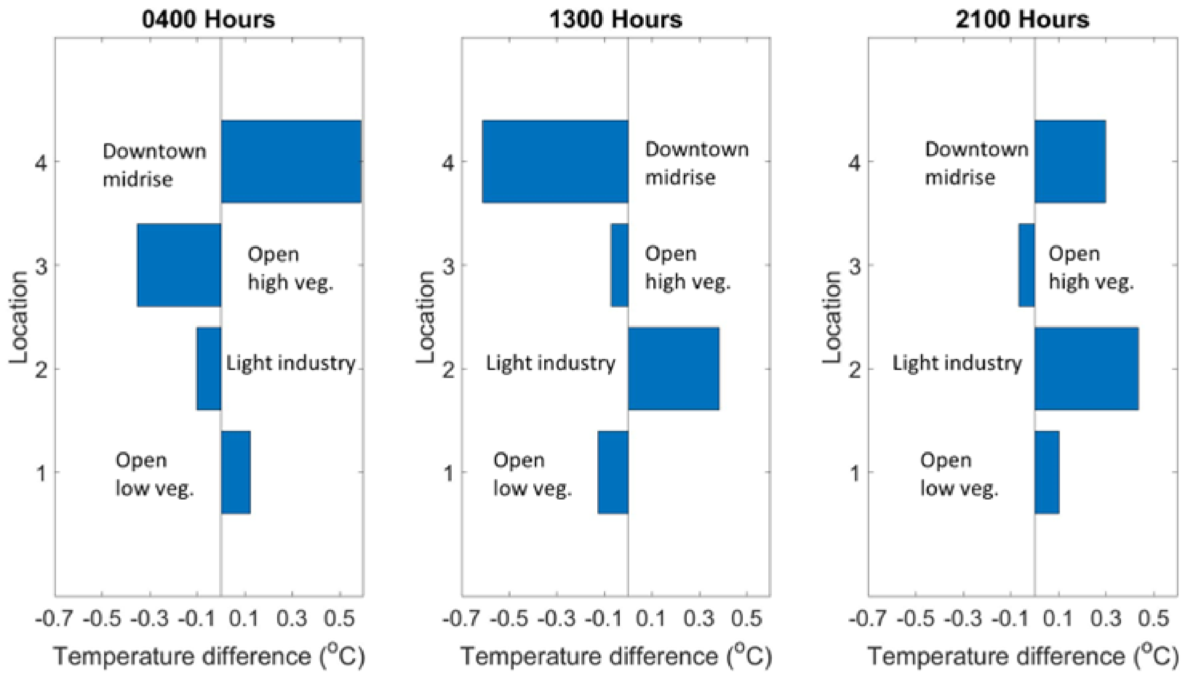

Figure 18: Diurnal temperature distribution for four LCZ on July 21, 2019.

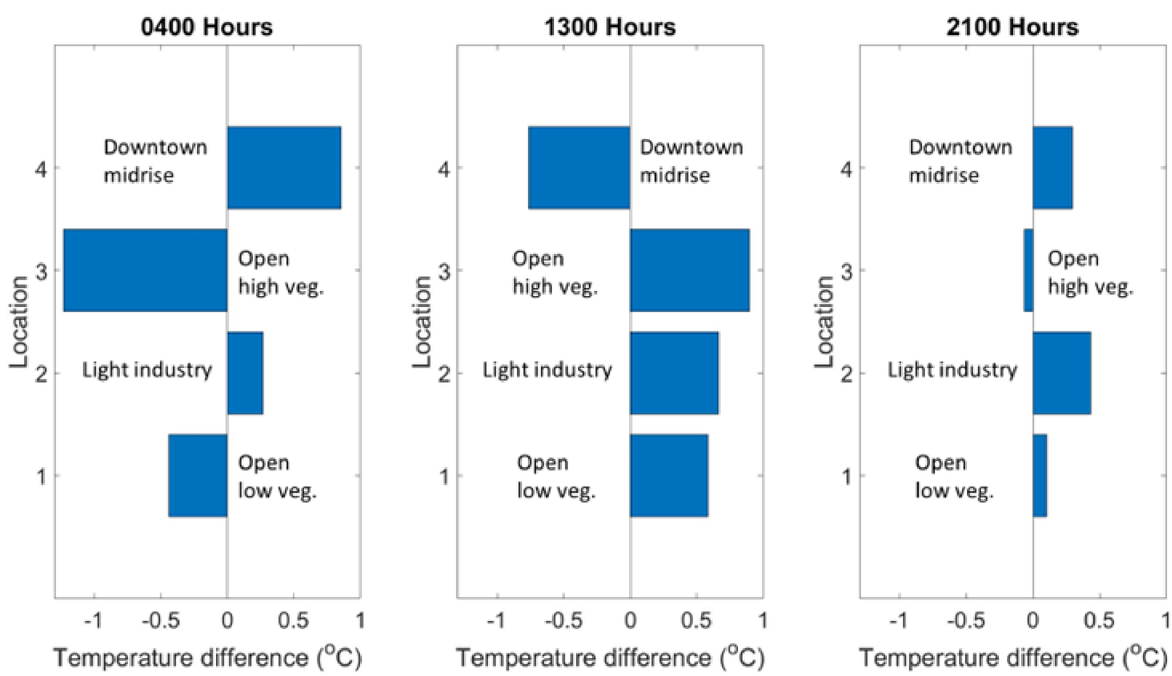

Figure 19: Diurnal temperature distribution for each LCZ on July 27, 2019.

The only LCZ to repeat the same pattern on both days is the downtown midrise. On July 21, this LCZ cools in the afternoon, returning to warm temperatures for the morning and evening (Figure 18). Similarly, on July 27, the same pattern is seen in the downtown LCZ. This is consistent with the cool temperature departure seen in Figure 10, of about 0.6 °C.

The open high vegetation LCZ has been consistently cool in all previous analysis. On July 21, the open high vegetation neighborhood experienced cool temperatures during all three measurement sessions, while the remaining three LCZs varied depending on time of day (Figure 18). However, unlike on July 21, on July 27 the open high vegetation neighborhood experienced warmer temperatures at 1300 hours but was below the city average for the remaining time slots (Figure 19).

Warm afternoon temperatures were discovered in Figure 10, which showed on average this LCZ is about 0.2 °C warmer than the transect mean in the afternoon. The open low vegetation neighborhood has warm temperature departures on the morning of July 21, but cool temperatures departures on July 27. It also has cool temperatures in the afternoon of July 21, but warm temperatures in the afternoon of July 27. Our results from Figure 10 show that this LCZ temperature departure is on average +0.16 °C, which could explain the slight variation to a cooler afternoon as it ranges close to the city average.

Discussion

The following is the ranking of LCZs from hottest to coolest LCZ in San José during the hours just after sunset: Downtown, Industry, Open Low Vegetation Neighborhood, Lake, Open

High Vegetation Neighborhood, Urban Park. The only analysis under which this order changed was the warm transect over 25 °C where the urban park was warmer than the lake and the open high vegetation neighborhood. The lake LCZ was most similar to the average temperature of the city.

Our results supported our hypothesis that higher temperatures would occur in the minimally vegetated neighborhood compared to the highly vegetated neighborhood regardless of similar urban form. This temperature difference is due to increased evapotranspiration and pervious ground surface. The pervious fraction in the high vegetation neighborhood was 62.5% more than in the low vegetation neighborhood and the latter was on average 0.5 °C hotter than the highly vegetated neighborhood.

Our results also supported the hypothesis that the highly vegetated neighborhood is expected to have cooler temperatures than other types of built urban form due to the high pervious ground fraction and vegetation density within this LCZ. This LCZ was the second coolest LCZ in San José and coolest of the built urban form.

Additionally, our results supported our hypothesis that the highest overall temperature in the city was expected to be produced by the densely built urban form of the downtown region, which was 0.6 °C above the transect mean (Figure 9). This LCZ has more buildings and surface area, a low pervious fraction, a high aspect ratio, and replaced the natural landscape, all of which causes increases in temperature.

Our results also showed that temperature differences were weakened during windier conditions due to increased mixing of air between LCZs (Figure 14 & Figure 15). However, temperature differences were not always strengthened under hotter background conditions.

Many general patterns observed in San José were consistent with findings in other urban climate studies (Yang et al., 2017), showing increased temperatures in dense and built urban forms and decreased temperatures in areas with higher vegetation or parklands (Spronken-Smith & Oke, 1998; Jansson et al., 2007; Bottyán et al., 2005; Szeged & Gyarmati 2009).

4.1 Local Climate Zone Classifications

In San José, the subclassification of E, bare rock or paved, was applied to four out of the six climate zones. Considering the lack of Csb climate representation in LCZ literature and the cultural and regional construction of San José, there is a pattern of increased paved surfaces which currently have no comparison. As suggested by Betchel et al. (2015), supervised LCZ design should be conducted with a local expert so that surface characteristics are incorporated and considered.

The industrial LCZ did not receive a subclassification even with an increased impervious fraction. A subclassification of E, bare rock or paved, would be repetitious as the primary land cover for LCZ 8 is already bare rock or paved. However, in Colombo, Sri Lanka, LCZ 8 was subclassified with E (Perera & Emmanuel, 2018). Without access to the LCZ measurement data or sufficient discussion on this particular decision, it is difficult to ascertain the intention behind this subclassification. Additionally, the framework suggests subclasses for LCZs which feature alternative urban forms to the parent classification and is not inherently clear if this situation would require a subclass.

The open low rise neighborhoods in San José did receive separate subclassifications of either B, for scattered trees, or E, for bare rock or paved. In Vancouver, British Colombia, Aminipouri et al. (2019), classified a LCZ 6_A, similar to San José's LCZ 6_B. This subclassification was prompted by terrain roughness class above the indicator (Aminipouri et al., 2018). In Nancy, France, LCZ 6 was subclassified with LCZ 9, sparsely built, to account for values which bordered between LCZ 6 and 9, such as a wider canyon aspect ratio and a decreased building surface fraction (Leconte et al., 2015). While the canyon aspect ratio in our LCZ 6s' are smaller than expected, the building percentage is not below the threshold of 20%.

In downtown San José, a subclassification of 1, high rise, and E, bare rock or paved was added to account for values outside of the indicators. Similarly, in Nanjing, China, a subclass of E was added to a LCZ 2 due to an increased impervious fraction of 61% (Yang et al., 2017). Subclassifications based on the mixing of building heights are common in studies such as in Londrina, Brazil, which found different combinations of compact LCZs 1,2, and 3 (Anjos et al., 2020).

Combinations of natural land cover types are not as common and the most comparable subclassification to San José is seen in Londrina, Brazil, which has a similar subclassification of LCZ G_A for dense trees (Anjos et al., 2020). Subclassification of E, bare rock or paved, was not found in this literature review for any of the three plant types: low plants, scattered trees, or dense trees. Even in Colombo, Sri Lanka, where 46 subclasses were assigned, there were no subclasses assigned to natural landscapes A-G (Perera & Emmanuel, 2018).

In this study, five out of ten LCZ indicators were explored: aspect ratio, building surface fraction, impervious surface fraction, pervious surface fraction, and height of roughness elements. Further confidence in the LCZ classification framework would need additional GIS analysis. Further research would consist of continued investigation and analysis of LCZ geometric surface cover properties and thermal, radiative, and metabolic processes listed in Table 1.

4.2 Park and Lake Cool Island Effects

Vegetated areas in LCZ research vary depending on eco region. Commonly surveyed LCZs include dense trees (A), scattered trees (B), and low plants (D). The PCI effect has been studied at length in conjunction with the growth of UHI research; expected results due to the PCI phenomena in both the framework and the hypothesis for this study included cooler temperatures in LCZ B, scattered trees, and the highly vegetated open low rise neighborhood LCZ 6_B (Stewart et al., 2012). The PCI effect for San José is 1.5 °C which is the temperature difference in the evenings between downtown, LCZ 2_{1E} and the urban park, LCZ $B_{E.}$ This PCI difference shows that areas with more vegetation and soil, such as LCZ B_E cooling faster and more effectively than the built urban surfaces which retain heat cool.

According to theory, evapotranspiration causes cooler temperatures compared to the built urban form which reduces the amount of vegetation and soil water storage. The urban park, LCZ B_E, did have the coolest temperatures in San José in the evening with an average temperature departure of 0.9 °C below the average due to vegetation fraction. Similarly, B, scattered trees, or A, dense trees, were found to be the coolest in Las Vegas, NV, Opelika, AL, Nanjing, China, and in Vancouver, BC (Stewart & Oke, 2012; Yang et al., 2017; Chieppa et al., 2018; Wang et al., 2018). LCZ D, low plants, was found to be the coolest vegetated LCZ in three studies, Dublin, Ireland, Phoenix, AZ, and Londrina, Brazil (Alexander & Mills, 2014; Wang et al., 2018; Anjos et al., 2020). Consistent with literature (Spronken-Smith & Oke, 1998; Jansson et al., 2007;

Bowler et al., 2012) and surface energy balance theory, vegetation provides a cool microclimate and is an option to combat urban heating.

Afternoon or daytime temperatures were provided for LCZ B in Phoenix, AZ, Las Vegas, NV, and both cities in Alabama. Unlike San José, all four cities saw cooler temperatures in LCZ B, below the average (Chieppa et al., 2018; Wang et al., 2018). Theoretically, LCZ B should have cooler temperatures however, it is possible that due to being a Mediterranean climate with less than 3% of precipitation falling in the summer months, that there is a lack of water availability. The lack of water availability during the daytime would hinder evapotranspiration and plants may have adapted to this climate and close their stoma to preserve energy during hot afternoons.

In the evenings, LCZ G, water, has the ability to be the coolest LCZ as seen in Las Vegas, NV with a 5 °C cooling from the average and in Londrina Brazil at 0.8 °C below the city average (Wang et al., 2018; Anjos et al., 2020). However, in Phoenix, AZ and Auburn, AL, LCZs with trees were as cool as or cooler than waterbodies (Chieppa et al., 2018; Wang et al., 2018). Similarly, in San José, the lake was not the coolest LCZ in the evenings, rather the urban park and highly vegetated neighborhood.

In San José, the lake, LCZ, produced a small positive temperature departure from the average in the evenings, similar to the lake in Las Vegas which produced a night temperature departure of 0.4 °C (Wang et al., 2018). This is counterintuitive to the energy budget since it is expected the lake surface would be dominated by Q_E and help cool the surrounding area, due to lower Q_H. Due to the lake size in San José, small and shallow, it is likely that this lake absorbed heat during the day and is slightly slower to cool than the surrounding surface area during the evenings, which would explain the result of a small positive temperature departure in Figure 9.

Wang et al. (2018) reported daytime temperature differences for LCZ G in Las Vegas and Phoenix. Similar to San José, daytime water measurements were the coolest in Phoenix and Las Vegas (Wang et al., 2018). In Phoenix, LCZ G had a pervious surface fraction of 93% and a temperature departure of 20 °C below the average (Wang et al., 2018). San José's afternoon temperature departure of LCZ G was only 1.5 °C most likely due to a smaller pervious surface fraction of 79% which also included ground and trees. Water absorbs heat throughout the day and has a high specific heat capacity, which causes the lake to take a longer time to warm than paved or ground surfaces. This would explain the cool temperature departures of water bodies during the daytime when Q_E is more prominent due to incoming Q^* as available energy and show that LCZ G could be a significant LCZ for people to find respite from daytime heat.

Overall, only two studies showed temperature deviations below the average in LCZ 6, in Phoenix, AZ with a negligible cooling of 0.1 °C and Vancouver, BC with a cooling of 0.4 K (Stewart & Oke, 2012; Wang et al., 2018). Neither of these locations had subclassifications. As expected, the highly vegetated open low rise neighborhood in San José showed cooling similar to land cover types A or B, rather than built forms reported in Table 2 due to evapotranspiration and increased water infiltration due to an abundance of pervious surface. Vegetation as a cooling factor has been addressed widely in the literature (Shashua-Bar & Hoffman, 2000; Bowler et al., 2012; Gunawardena et al., 2017) and this neighborhood in San José shows a measurable impact of vegetation to combat urban heating.

4.3 The Built Urban Form and UHI

Downtown San José has the highest average temperature departure in the evenings in agreement with theory and previous studies (e.g. Table 2) which show the increase of urban materials and the replacement of the natural landscape causes an increase in temperature. These increases in the built urban form lead to increased temperatures and the UHI from the absorption of additional heat which is penetrated into the urban materials during the day which alters the SEB (Oke, 1987). Downtown is the densest LCZ in San José and has the largest surface area, largest impervious fraction, and is able to absorb more heat than smaller buildings. Likewise, LCZs 1 and 2 report the most warming or highest UHI intensity in every study surveyed that reported compact high rise or midrise LCZs (Table 2). Londrina, Brazil produced the same warming as San José (0.6 °C) for compact midrise urban form (Anjos et al., 2020). In Dublin, Ireland, LCZ 2 reported a 2.1 °C temperature departure above the average and was the hottest LCZ in the study (Alexander & Mills, 2014). In Kochi, India, the compact midrise LCZ was 2.8 °C warmer than the lightweight low rise zone (Thomas et al., 2014).

Downtown is consistently the coolest LCZ in the afternoon (Figure 13). According to UHI literature, increases in density of buildings and increases of the built urban form lead to the UHI especially in the evenings, but also in the afternoons in highly urbanized areas or urban centers (Gedzelman et al., 2003; Giridharan et al., 2004). This LCZ was expected to be above the city average and we are unable to fully explain the consistent negative temperature departure in this LCZ. Possible reasons include this LCZ being the northmost location with winds blowing from the Bay across the airport cooling the downtown region more effectively than the neighborhoods sampled to the south. Another possibility is shading caused by multistory buildings coupled with the absorption of incoming radiation into urban materials or increased surface roughness due to a mix of building heights from midrise to high rise. Additional afternoon temperature samples would be required to further investigate this pattern. Absorption of incoming Q* during the day does lead to the fact that this LCZ had the highest temperatures at night due to the release of the stored heat from the day.

The industry zone has higher temperatures in the evenings than most other LCZs due to large impervious fraction, building surface fraction, and building area. Only LCZ 2 in San José, downtown midrise, had a larger temperature departure due to an increase in building density and stories. Building surface area, fraction, and impervious fraction increase temperature due to the replacement of the natural environment and changes in the SEB due the increase of urban materials which absorb heat during the day and release it in the evening (Oke, 1987). LCZ 8s consistently produce second highest temperature departures following compact high rise or compact midrise LCZs (Table 2). Studies which did not report LCZ 1 or 2, such as Wang et al. (2018), show large low rise as the hottest LCZs. In Las Vegas, NV and Phoenix AZ, LCZ 8 was around 1 °C above the city average (Wang et al., 2018). Similar to San José, Londrina, Brazil showed a temperature departure of 0.4 °C above the average in LCZ 8 (Anjos et al., 2020). In Chongqing, China, LCZ 8 was 0.7 °C cooler than LCZ 1 (Wang et al., 2017).

The industrial LCZ was similar to its evening departure in the afternoons. Even with increased building surface area and paved surfaces throughout this LCZ, there are still large gaps between buildings with an aspect ratio of 0.17 compared to downtown's 0.76. This allows for greater release of heat at night in the industrial area compared to the more compact downtown.

Temperatures in LCZ 6 are, on average, cooler than those in LCZ 2 or 8 which is comparably seen in Dublin, Ireland where temperatures in LCZ 6 were 1.13 °C cooler than in LCZ 2, close to San José's LCZ 6_B and LCZ 2_{1E} (Alexander & Mills, 2014). LCZ 6 replaces some of the natural landscape with built environment, but on average, LCZ 6 has smaller building surface fractions, building surface area, and impervious fractions than LCZ 2 or 8. LCZ 6 usually has higher vegetation fractions than LCZ 2 or 8 and smaller aspect ratios. In agreement with theory, LCZ 6 in San José was cooler than 2 and 8, due to smaller building surface fractions and decreased building surface area which cannot absorb as much incoming radiation as other LCZs with increased amounts of built urban form (Oke, 1987).

Reported temperature departures in LCZ 6 were as high as 1.92 °C in Kochi, India or can be below the average such as seen in Vancouver, BC with a cooling of 0.4 K which is most similar to San José LCZ 6B (Stewart & Oke, 2012; Thomas et al., 2014). The open low-rise classification is meant to have an abundance of pervious land cover in addition to building materials and concrete (Stewart & Oke, 2012). Therefore, temperature differences or UHI intensities from the city average are not as large as LCZs 1, 2, or 8 which have buildings with larger surface area and increased impervious surface fraction.

Open low-rise neighborhoods vary in the studies surveyed. Most LCZ 6 were found to be warmer than average temperatures or have a positive UHI intensity, such as in Las Vegas, NV and Auburn, AL at 0.3 °C which was the same as LCZ 6_E in San José (Chieppa et al., 2018; Wang et al., 2018). LCZ 6_E produced warmer temperatures than LCZ 6_B due to vegetation differences. Because of this, increasing vegetation in urban areas has been noted as an effective practice to mitigate the UHI (Bowler et al., 2012; Gunawardena et al., 2017).

In Dublin, LCZ 6 had a temperature difference of 0.97 °C above the average, unlike LCZ 6_B, while the LCZ 2 had a temperature above the average at 2.1 °C (Alexander & Mills, 2014). In Kochi, India and Nancy, France, the open low rise LCZs were both nearly 2 °C cooler than the compact midrise LCZs (Thomas et al., 2014; Leconte et al., 2015). These locations in France and India come from different climates and yet still have similar temperature differences, showing support for the universal nature of the LCZ classification system.

The increased impervious fraction in LCZ 6_E, the open low vegetation neighborhood, caused this LCZ to have similar temperatures to the LCZ 8, industry. These LCZs were not statistically significantly different from each other in San José most likely due to high impervious percentage in both LCZs (Table 4). In Las Vegas, LCZ 6 had a similar temperature departure to LCZ 6E in San José of 0.3 °C and was 0.8 °C cooler than LCZ 8 (Wang et al., 2018). However, the open high vegetation neighborhood, LCZ 6_B, was statistically different with a temperature difference of 0.7 °C, similar to the 0.8 °C in Las Vegas, NV (Wang et al., 2018).

In the daytime, the open high and open low vegetation neighborhoods are similar in temperature with absorption of heat into building materials occurring during the day. The open high vegetation neighborhood would have been expected to be lower in temperature due to an increased amount in vegetation, but like the urban park, both LCZs have temperature departures above the mean in the afternoons. Possibly, this may be due to a lack of water availability to support evapotranspiration in a Mediterranean climate like San José or due to the type of plants in San José and their stomatal reactions to these microclimates.

Our findings that windier conditions produced a decreased range of temperature departures was similarly seen in Londrina, Brazil, where synoptic patterns were investigated including winds above 4.0 m s^{-1} (Anjos et al., 2020). Similar to San José, temperature departures decreased overall, and temperature differences were weaker in Londrina Brazil (Anjos et al., 2020). Stronger winds produced a temperature difference of 0.5 °C between the lake with dense trees and compact midrise in Brazil and a 1.2 °C difference between these LCZs with weaker winds, averaging 2.1m s^{-1} (Anjos et al., 2020). The likely reason for lower temperature heterogeneity under windier conditions is caused by the enhancing mixing of air parcels between neighborhoods.

Conclusions

This study explored the LCZ classification framework as a means to investigate temperature variation in the built urban form using mobile vehicle measurements in San José, California. The LCZ framework and subclassification of the built urban form allows for comparison of LCZs worldwide based on the variation of the built urban form and our results support LCZ classification as temperature departures are similar in the same built urban forms from different climates. In San José, densely built urban form, specifically the downtown region, had the highest temperatures relative to all other LCZs. Results show consistent warm temperatures in the evenings in the downtown midrise LCZ at 0.6 °C above the transect mean.

The coolest temperatures at 0.9 °C below the transect mean were in the urban park under typical summer conditions in San José. The urban park was consistently the coolest LCZ with the open high vegetation neighborhood consistently as the second coolest LCZ. The cooler temperatures in San José are found in areas which have increased vegetation and increased pervious surfaces which allow for cooling via evapotranspiration and soil water storage. These areas with additional vegetation and soil produce cooling within the city as seen by our negative temperature departure of the urban park and open high vegetation neighborhood.

We effectively compared vegetation differences in the open low rise neighborhoods and demonstrated the importance of vegetation as a cooling component in the built urban form. Despite their similarity in LCZ characteristics, especially in the built environment, the difference in pervious fractions showed significant temperature differences between neighborhoods. Subclassification of these neighborhoods showed similar results to theory based on vegetation amounts and characteristics of the built urban form where the high vegetation neighborhood produced a temperature departure below the mean and the low vegetation neighborhood temperature departure above the mean. With a pervious fraction of 67%, the highly vegetated single family home neighborhood was on average 0.5 °C cooler than the single family neighborhood with a pervious fraction of 4.5%.

We found that temperature differences were weakened under windier conditions due to enhanced mixing caused by winds. Although, temperature differences were not always strengthened under hotter weather conditions. Unlike the evenings, the diurnal measurements show different patterns. In the afternoon, the downtown midrise is below the city average whereas the urban park is the warmest LCZ contrary to their evening patterns. The lake was consistently around the city average during the evening transects, with the coolest temperatures midday.

Suggested further exploration would continue GIS investigation to obtain the additional five geometric, thermal, radiative, and metabolic properties not found in this study. These values would provide more descriptive results of LCZs in San José to allow for further comparison of LCZs worldwide based on these additional properties.

Future exploration of LCZs in San José should include increased collection of afternoon temperature data to better explain diurnal patterns and to confirm the unusual downtown cool island. Additional temperature departure information could be obtained under varying synoptic conditions such as following rain events, and during different seasons. Additional sampling of these conditions and time frames would allow for confident and meaningful conclusions since there were limited samples of afternoon, morning, and hot background conditions and no sampling was done outside of summer.

Climate change scenario modeling based on projected temperature increases and the temperature differences of LCZs could be conducted to analyze future predictions of urban heating based on the built urban form. Evidence from this study suggests that the UHI effect is exacerbated under hotter background conditions. In addition, satellite imagery could be used to better inform land use and heating differences across San José and could be compared to the field measurements obtained during this study.

More neighborhoods in San José could be identified for additional LCZs temperature surveys such as compact low or midrise condominiums or apartment homes or mixed use development such as residential and retail. Additional LCZ identification and surveys would allow for a more complete accounting of San José's microclimate variability.

This study provides a unique sample of a city in a Mediterranean climate using the LCZ framework. This study, therefore, added a previously unexplored climate type, Csb, to build on the global datasets already generated. Combined, these findings are critical to informing city planning and urban design in a changing global climate, particularly with consideration for human health and thermal comfort.

References

Alexander, P. J., & Mills, G. (2014). Local climate classification and Dublin's urban heat island. *Atmosphere*, 5(4), 755–774. https://doi.org/10.3390/atmos5040755

Aminipouri, M., Rayner, D., Lindberg, F., Thorsson, S., Knudby, A. J., Zickfeld, K., Middel, A., & Krayenhoff, E. S. (2019). Urban tree planting to maintain outdoor thermal comfort under climate change: The case of Vancouver's local climate zones. *Building and Environment*, 158(February), 226–236. https://doi.org/10.1016/j.buildenv.2019.05.022

Anjos, M., Targino, A. C., Krecl, P., Oukawa, G. Y., & Braga, R. F. (2020). Analysis of the urban heat island under different synoptic patterns using local climate zones. *Building and Environment*, 185(August). https://doi.org/10.1016/j.buildenv.2020.107268

Bechtel, B., Alexander, P. J., Böhner, J., Ching, J., Conrad, O., Feddema, J., Mills, G., See, L., & Stewart, I. (2015). Mapping local climate zones for a worldwide database of the form and function of cities. *ISPRS International Journal of Geo-Information*, 4(1), 199–219. https://doi.org/10.3390/ijgi4010199

Bechtel, B., Demuzere, M., Mills, G., Zhan, W., Sismanidis, P., Small, C., & Voogt, J. (2019). SUHI analysis using Local Climate Zones—A comparison of 50 cities. *Urban Climate*, 28(January), 100451. https://doi.org/10.1016/j.uclim.2019.01.005

Bechtel, B., Demuzere, M., Sismanidis, P., Fenner, D., Brousse, O., Beck, C., Van Coillie, F., Conrad, O., Keramitsoglou, I., Middel, A., Mills, G., Niyogi, D., Otto, M., See, L., & Verdonck, M.-L. (2017). Quality of Crowdsourced Data on Urban Morphology—The Human Influence Experiment (HUMINEX). *Urban Science*, 1(2), 15. https://doi.org/10.3390/urbansci1020015

Bottyán, Z., Kircsi, A., Szegedi, S., & Unger, J. (2005). The relationship between built-up areas and the spatial development of the mean maximum urban heat island in Debrecen, Hungary. International Journal of Climatology, 25(3), 405–418. https://doi.org/10.1002/joc.1138

Bowler, D. E., Buyung-Ali, L., Knight, T. M., & Pullin, A. S. (2010). Urban greening to cool towns and cities: A systematic review of the empirical evidence. *Landscape and Urban Planning*, 97(3), 147–155. https://doi.org/10.1016/j.landurbplan.2010.05.006

Chieppa, J., Bush, A., & Mitra, C. (2018). Using '"Local Climate Zones"' to detect urban heat island on two small cities in Alabama. *Earth Interactions*, 22(16). https://doi.org/10.1175/EI-D-17-0020.1

Dahl, K., Licker, R., Abatzoglou, J.T., & Declet-Barreto, J. (2019). Increased frequency of and population exposure to extreme heat index days in the United States during the 21st century. *Environmental Research Communications*, 1(7). https://doi.org/10.1088/2515-7620/ab27cf

Demuzere, M., Bechtel, B., & Mills, G. (2019). Global transferability of local climate zone models. *Urban Climate*, 27(February 2018), 46–63. https://doi.org/10.1016/j.uclim.2018.11.001

Department of Planning (2014). Fact Sheet: History and Geography. San José Department of Planning: Building & Code Enforcement. http://www.sanjoseca.gov/index.aspx?NID=2044

Gago, E. J., Roldan, J., Pacheco-Torres, R., & Ordóñez, J. (2013). The city and urban heat islands: A review of strategies to mitigate adverse effects. *Renewable and Sustainable Energy Reviews*, 25, 749–758. https://doi.org/10.1016/j.rser.2013.05.057

Gedzelman, S. D., Austin, S., Cermak, R., Stefano, N., Partridge, S., Quesenberry, S., & Robinson, D. A. (2003). Mesoscale aspects of the Urban Heat Island around New York City. Theoretical and Applied Climatology, 75(1–2), 29–42. https://doi.org/10.1007/s00704-002-0724-2

Giridharan, R., Ganesan, S., & Lau, S. S. Y. (2004). Daytime urban heat island effect in high-rise and high-density residential developments in Hong Kong. Energy and Buildings, 36(6), 525–534. https://doi.org/10.1016/j.enbuild.2003.12.016

Google Earth Pro. 2020.

Grimmond, C. S. B. (2006). Progress in measuring and observing the urban atmosphere. *Theoretical and Applied Climatology*, 84(1–3), 3–22. https://doi.org/10.1007/s00704-005-0140-5

Gunawardena, K. R., Wells, M. J., & Kershaw, T. (2017). Utilising green and bluespace to mitigate urban heat island intensity. *Science of the Total Environment*, 584–585, 1040–1055. https://doi.org/10.1016/j.scitotenv.2017.01.158

Iamarino, M., Beevers, S., & Grimmond, C. S. B. (2012). High-resolution (space, time) anthropogenic heat emissions: London 1970-2025. *International Journal of Climatology*, 32(11), 1754–1767. https://doi.org/10.1002/joc.2390

Jansson, C., Jansson, P. E., & Gustafsson, D. (2007). Near surface climate in an urban vegetated park and its surroundings. Theoretical and Applied Climatology, 89(3–4), 185–193. https://doi.org/10.1007/s00704-006-0259-z

Kleerekoper, L., Van Esch, M., & Salcedo, T. B. (2012). How to make a city climate-proof, addressing the urban heat island effect. *Resources, Conservation and Recycling*, 64, 30–38. https://doi.org/10.1016/j.resconrec.2011.06.004

Kotharkar, R., & Bagade, A. (2018). Evaluating urban heat island in the critical local climate zones of an Indian city. *Landscape and Urban Planning*, 169(August 2017), 92–104. https://doi.org/10.1016/j.landurbplan.2017.08.009

Leconte, F., Bouyer, J., Claverie, R., & Pétrissans, M. (2015). Using Local Climate Zone scheme for UHI assessment: Evaluation of the method using mobile measurements. *Building and Environment*, 83, 39–49. https://doi.org/10.1016/j.buildenv.2014.05.005

Lehnert, M., Geletič, J., Husák, J., & Vysoudil, M. (2015). Urban field classification by "local climate zones" in a medium-sized Central European city: the case of Olomouc (Czech Republic). *Theoretical and Applied Climatology*, 122(3–4), 531–541. https://doi.org/10.1007/s00704-014-1309-6

Miller, M. (1999). Climate of San José. *NOAA Technical Memorandum*.

Morgan, D., Myrup, L., Rogers, D., & Baskett, R. (1977). Microclimates within an Urban Area. *Annals of the Association of American Geographers,* Mar., 1977, Vol. 67, No. 1. https://www.jstor.org/stable/2562241

Multi- Resolution Land Characteristics Consortium. 2020. *National Land Cover Database (NLCD*) Retrieved October 15, 2020 from https://www.mrlc.gov/data?f%5B0%5D=category%3ALand%20Cover&f%5B1%5D=category%3AUrban%20Imperviousness

National Climate Data Center. 2020. National Centers for Environmental Information. *National Oceanic and Atmospheric Administration.* Retrieved June 6, 2020 from https://www.ncdc.noaa.gov/

Norton, B. A., Coutts, A. M., Livesley, S. J., Harris, R. J., Hunter, A. M., & Williams, N. S. G. (2015). Planning for cooler cities: A framework to prioritise green infrastructure to mitigate high temperatures in urban landscapes. *Landscape and Urban Planning*, 134, 127–138. https://doi.org/10.1016/j.landurbplan.2014.10.018

Offerle, B., Grimmond, C. S. B., & Oke, T. R. (2003). Parameterization of net all-wave radiation for urban areas. *Journal of Applied Meteorology*, 42(8), 1157–1173. https://doi.org/10.1175/1520-0450(2003)042<1157:PONARF>2.0.CO;2

Oke, T. R. 1987. *Boundary Layer Climates*. 2nd Ed. Routledge.

Oke, T. R. (2006). Initial guidance to obtain representative meteorological observations at urban sites. *World Meteorological Organization: Instruments and Observing Methods.* 81. https://doi.org/10.1007/s12028-011-9538-3

Oke, T. R. (1988). The urban energy balance. *Progress in Physical Geography*, 12(4), 471–508. https://doi.org/10.1177/030913338801200401

Oke, T. R. (2006). Towards better scientific communication in urban climate. *Theoretical and Applied Climatology*, 84(1–3), 179–190. https://doi.org/10.1007/s00704-005-0153-0

Perera, N. G. R., & Emmanuel, R. (2018). A "Local Climate Zone" based approach to urban planning in Colombo, Sri Lanka. *Urban Climate*, 23, 188–203. https://doi.org/10.1016/j.uclim.2016.11.006

Sakakibara, Y., & Matsui, E. (2005). Relation between heat island intensity and city size indices/urban canopy characteristics in settlements of Nagano basin, Japan. *Geographical Review of Japan*, 78(12), 812–824. https://doi.org/10.4157/grj.78.812

San José CA GIS Open Data. 2020. Building Footprint. *geo.sanjoseca.gov*. Retrieved October 1, 2020 from https://gisdata-csj.opendata.arcgis.com/datasets/building-footprint?geometry=-122.541%2C37.110%2C-121.159%2C37.493

Shashua-Bar, L., & Hoffman, M. E. (2000). Vegetation as a climatic component in the design of an urban street. *Energy and Buildings*, 31(3), 221–235. https://doi.org/10.1016/S0378-7788(99)00018-3

Skarbit, N., Stewart, I. D., Unger, J., & Gál, T. (2017). Employing an urban meteorological network to monitor air temperature conditions in the 'local climate zones' of Szeged, Hungary. *International Journal of Climatology*, 37(March), 582–596. https://doi.org/10.1002/joc.5023

Spronken-Smith, R. A., & Oke, T. R. (1998). The thermal regime of urban parks in two cities with different summer climates. *International Journal of Remote Sensing*, 19(11), 2085–2104. https://doi.org/10.1080/014311698214884

Stevan, S., Dragan, M., Lazar, L., Vladimir, M., Daniela, A., & Dragoslav, P. (2013). Classifying urban meteorological stations sites by "local climate zones": Preliminary results for the City of Novi Sad (Serbia). *Geographica Pannonica*, 17(3), 60–68.

Stewart, I. D., & Oke, T.R. (2012). Datasheets for Local Climate Zones, 93(12). https://doi.org/10.1175/BAMS-D-11-00019.2

Stewart, I. D., & Oke, T.R. (2012). Local Climate Zones for Urban Temperature Studies. *American Meteorological Society*. JSTOR 93(12), 1879-1900.

Szeged, S., & Gyarmati, R., (2009). Impacts of Urban Green Spaces on the Spatial Structure of the Urban Heat Island in Debrecen and Different Sized Settlements in its Neighborhood. Acta Climatologcia Chorologica, 42-43, 151-158.

Terjung, W.H. and Collaborators. (1970). The Energy Balance Climatology of a City-Man System. *Annals of the Association of American Geographers*, Sep., 1970 , Vol. 60 , No. 3. https://www.jstor.org/stable/2561671

Terjung W.H., & Louie, S.S. (1973). Solar Radiation and Urban Heat islands. *Annals of the Association of American Geographers*, Jun., 1973, Vol. 63, No. 2. https://www.jstor.org/stable/2562269

Thomas, G., Sherin, A. P., Ansar, S., & Zachariah, E. J. (2014). Analysis of Urban Heat Island in Kochi, India, Using a Modified Local Climate Zone Classification. *Procedia Environmental Sciences*, 21, 3–13. https://doi.org/10.1016/j.proenv.2014.09.002

United Nations. "68% Of the World Population Projected to Live in Urban Areas by 2050, Says UN | UN DESA Department of Economic and Social Affairs." *United Nations*, United Nations, 16 May 2018, www.un.org/development/desa/en/news/population/2018-revision-of-world-urbanization-prospects.html.

Whitman, S., Good, G., Donoghue, E.R., Benbow, N., Shou, W., & Mou, S., (1997) Morality in Chicago attributed to the July 1995 heat wave. *American Journal of Public Health*, 87(9), 1515-1518.

Wang, C., Middel, A., Myint, S. W., Kaplan, S., Brazel, A. J., & Lukasczyk, J. (2018). Assessing local climate zones in arid cities: The case of Phoenix, Arizona and Las Vegas, Nevada. *ISPRS Journal of Photogrammetry and Remote Sensing*, 141, 59–71. https://doi.org/10.1016/j.isprsjprs.2018.04.009

Wong, N. H., & Yu, C. (2005). Study of green areas and urban heat island in a tropical city. *Habitat International*, 29(3), 547–558. https://doi.org/10.1016/j.habitatint.2004.04.008

Xue, J., You, R., Liu, W., Chen, C., & Lai, D. (2020). Applications of local climate zone classification scheme to improve urban sustainability: A bibliometric review. *Sustainability*, 12(19), 1–14. https://doi.org/10.3390/su12198083

Yang, X., Yao, L., Zhu, C., Jin, T., & Peng, L. L. (2017). Analysis of Local Heat Islands in Nanjing, China, based on the Local Climate Zone Scheme. *Procedia Engineering*, 205, 2501–2508. https://doi.org/10.1016/j.proeng.2017.09.980

Appendices

Appendix A: Evening pairwise comparisons of temperature differences between LCZs with P Values indicating significant or not significant differences between LCZs.

Location Comparison	Absolute Temperature Difference (° C)	P Value
Lake & Open Low Vegetation Neighborhood	0.12	0.9651
Lake & Urban Park	0.9	0.0001
Lake & Industry	0.36	0.1031
Lake & Open High Vegetation Neighborhood	0.37	0.0795
Lake & Downtown	0.59	0.0006
Open Low Vegetation Neighborhood & Urban Park	1.01	0.0001
Open Low Vegetation Neighborhood & Industry	0.25	0.4584
Open Low Vegetation Neighborhood & Open High Vegetation Neighborhood	0.48	0.0086
Open Low Vegetation Neighborhood & Downtown	0.48	0.0092
Urban Park & Industry	1.26	0.0001
Urban Park & Open High Vegetation Neighborhood	0.53	0.0027
Urban Park & Downtown	1.49	0.0001
Industry & Open High Vegetation Neighborhood	0.73	0.0001
Industry & Downtown	0.23	0.5329
Open High Vegetation Neighborhood & Downtown	0.96	0.0001

Appendix B: Afternoon pairwise comparisons of temperature differences between LCZs with P Values indicating significant or not significant differences between LCZs

Location Comparison	Absolute Temperature Difference (° C)	P Value
Lake & Open Low Vegetation Neighborhood	1.6	0.0001
Lake & Urban Park	2.79	0.0001
Lake & Industry	1.79	0.0001
Lake & Open High Vegetation Neighborhood	1.65	0.0001
Lake & Downtown	0.85	0.0297
Open Low Vegetation Neighborhood & Urban Park	1.17	0.0014
Open Low Vegetation Neighborhood & Industry	0.17	0.9831
Open Low Vegetation Neighborhood & Open High Vegetation Neighborhood	0.03	0.9999
Open Low Vegetation Neighborhood & Downtown	0.77	0.0564
Urban Park & Industry	1.0	0.0071
Urban Park & Open High Vegetation Neighborhood	1.14	0.0019
Urban Park & Downtown	1.94	0.0001
Industry & Open High Vegetation Neighborhood	0.14	0.9938
Industry & Downtown	0.94	0.0124
Open High Vegetation Neighborhood & Downtown	0.81	0.0423